

## **EUROPEAN COMMISSION**

HORIZON 2020 PROGRAMME - TOPIC H2020-GV-05-2017  
Electric vehicle user-centric design for optimised energy efficiency

GRANT AGREEMENT No. 769902



Design OptiMisation for efficient electric vehicles based on a  
USer-centric approach

### **DOMUS – Deliverable Report**

D1.5 Efficient Cabin Model for Simulating Thermal and  
Acoustic Behaviour of Car Cabins

<b>Deliverable No.</b>	DOMUS D1.5	
<b>Related WP</b>	WP1	
<b>Deliverable Title</b>	Efficient Cabin Model for Simulating Thermal and Acoustic Behaviour of Car Cabins	
<b>Deliverable Date</b>	2020-04-30	
<b>Deliverable Type</b>	REPORT	
<b>Dissemination level</b>	Public (PU)	
<b>Written By</b>	James Brusey (COV) Matteo Rostagno (CRF)	2020-03-12 2020-04-30
<b>Checked by</b>	James Brusey (COV)	2020-05-06
<b>Reviewed by (if applicable)</b>	Sebastian Möller (ViF)	2020-05-12 2020-05-21
<b>Approved by</b>	IDIADA	2020-05-22
<b>Status</b>	Final	2020-05-22

### Change Log

Version	Modifications of document	Author	Date
1	Creation of the document: table of contents, section headings, raw input in some sections (experimentation package, grant agreement, email exchanges)	James Brady	2020-02-13
2	Initial writing for public and sec 6	James Brusey	2020-03-12
3	Integrated input from CRF secs 5 & 7	James Brady	2020-03-23
4	Input from CRF in sections 1.4 and 7.1	James Brady	2020-04-14
5	New section 4.2 for general methodology to include reporting simulation accuracy	James Brusey	2020-04-15
6	Changes to template format and layout. Inclusion of new chapter (Chapter 4 in this version) "Purpose of the document" to be completed.	James Brady	2020-04-19
7	Remove numbering from all section headings before Chapter 1 "Purpose of Document"	James Brady	2020-04-22
8	Revise chapter 4	James Brusey	2020-04-24
9	Revised according to comments	Matteo Rostagno	2020-04-30
10	Inclusion of RMSE and NRMSE results	Matteo Rostagno	2020-05-06
11	Revision as per review	James Brusey and Matteo Rostagno	2020-05-14
12	Minor adjustment of explanation of delays	Alberto Merlo	2020-05-20

## *Disclaimer/ Acknowledgment*



Copyright ©, all rights reserved. This document or any part thereof may not be made public or disclosed, copied or otherwise reproduced or used in any form or by any means, without prior permission in writing from the DOMUS Consortium. Neither the DOMUS Consortium nor any of its members, their officers, employees or agents shall be liable or responsible, in negligence or otherwise, for any loss, damage or expense whatever sustained by any person as a result of the use, in any manner or form, of any knowledge, information or data contained in this document, or due to any inaccuracy, omission or error therein contained.

All Intellectual Property Rights, know-how and information provided by and/or arising from this document, such as designs, documentation, as well as preparatory material in that regard, is and shall remain the exclusive property of the DOMUS Consortium and any of its members or its licensors. Nothing contained in this document shall give, or shall be construed as giving, any right, title, ownership, interest, license or any other right in or to any IP, know-how and information.

This project has received funding from the European Union's Horizon 2020 research and innovation programme under grant agreement No 769902. The information and views set out in this publication does not necessarily reflect the official opinion of the European Commission. Neither the European Union institutions and bodies nor any person acting on their behalf, may be held responsible for the use which may be made of the information contained therein.

## Publishable Summary

### Background

The aim of this deliverable is to provide an efficient implementation of a thermal cabin model that can be used to rapidly and virtually assess cabin comfort making use of the assessment framework (D1.2) and the holistic comfort model (D1.3).

This deliverable aims to resolve a conflict that often occurs in computer aided engineering and design. Specifically, the need for accuracy and spatial resolution is in conflict with the computational speed required to optimize a system within a reasonable amount of time and using available computer resources.

In this case, high accuracy and spatial resolution is provided by simulating the car cabin thermal environment with computational fluid dynamic (CFD) simulation. For this project, the CFD model has been produced and validated as part of task 1.3 resulting in deliverable D1.4.

This high accuracy simulation typically takes around 10 minutes (elapsed time) to compute one second of transient simulation.

DOMUS, however, calls for much faster simulation for several key reasons:

1. The assessment framework requires simulation of 28 different scenarios that vary in length between 10 minutes to 30 minutes and thus the total simulation time for a *single assessment* is considerable.
2. Machine learning approaches that learn control algorithms such as Reinforcement Learning tend to require *months* or even *years* of simulation time to converge to the optimal solution.
3. Machine learning approaches that can evolve optimal cabin configurations may first require re-learning the control algorithm (point 2) for every new configuration and even then require thousands of assessments (point 1) to arrive at the optimal configuration.

Despite this severe contrast between the computational speed possible for high accuracy simulation and the computational speed required for full optimization, there is some cause for hope. This hope stems, firstly, from the possibility of using machine learning to approximate the high accuracy simulation and, secondly, the realization that a perfect simulation may not be needed to perform optimization on such things as the HVAC control algorithm.

Alongside work to speed up the CFD simulation (produced in Task 1.3), a back-up plan of using a 1D cabin model is also pursued. By 1D cabin model, we mean a model that is based on “lumped thermal capacity” that uses simplifying assumptions to produce approximate but reasonably fast thermal simulation.

This additional work provides a check and a safeguard. It is a check in the sense that the final accepted simulation should be at least comparable or better than the 1D simulator in terms of accuracy and computational speed. Thus, results for the 1D simulator are needed to perform this check.

Producing a 1D cabin model also safeguards the overall aims of the project by providing mitigation for the risk that the machine-learned approach fails to produce a sufficiently capable simulator.

### Task objectives

The objectives of the sub-task carried out are the following.

1. Produce a machine-learned simulation of the thermal aspects of the car cabin focusing on those aspects needed to assess thermal comfort.
2. Produce a 1D thermal cabin simulation model focusing on the same aspects.
3. Compare the two models in terms of their accuracy against the CFD simulation provided in D1.4

4. Compare the two models in terms of their accuracy against available measurement data produced in a climatic wind tunnel.
5. Compare the two models in terms of simulation performance on roughly equivalent computational hardware.

## Methods

All involved partners in the task engaged with defining overall methods through regular teleconference and face to face workshops (activity started as part of T1.4).

The methods consist of:

- Ordinary 1D modelling of the car cabin using AMESIM or GTSuite
- Machine learning to map current state and control values into next state values.

## Results

The key results include:

1. The machine learnt cabin model has an average normalized RMSE over all sensors of 1.8%. The RMSE for the average air temperature for the front bench is 0.4 K (0.8%) over all trials.
2. The machine learnt cabin model computes a second of simulation time in  $5.44 \times 10^{-6}$  s.
3. The machine learnt cabin model is able to interface to the holistic comfort model and, in comparison with the CWT data, gives a misclassification rate that ranges from 1.3% to 3.4%.
4. The 1D cabin model predicts the cabin average air temperature within  $\pm 1$  K (1.52%) with respect to the reference temperature.
5. The 1D cabin model predicts AC pressure with an average error less than 0.6 bar (3%) at high pressure and 0.1 bar (6%) (steady state) at low pressure
6. The 1D cabin model computes a second of simulation time in 0.25 s (worst case – when the AC compressor is on) or 0.0076 s (AC compressor off).

These results meet the requirements set out in the objectives for this part of the project and provide a strong foundation for the remainder of the DOMUS work to build upon.

## Contents

1	Purpose of the document.....	11
1.1	Document structure .....	11
1.2	Deviations from the original description in the Grant Agreement Annex 1- Part A.....	11
	Description of work related to deliverable in GA Annex 1 – Part A .....	11
	Time deviations from original planning in GA Annex 1 – Part A .....	12
	Content deviations from original planning in GA Annex 1 – Part A .....	12
2	Introduction (COV/CRF).....	13
2.1	Objectives .....	13
2.2	Relationship to DOMUS objectives.....	13
2.3	Relationship to other work packages and tasks .....	13
2.4	Methodology common to both approaches.....	14
	Error reporting.....	14
3	Efficient 1D model using traditional methods (CRF) .....	16
3.1	Methods for obtaining the model .....	16
3.2	Model description.....	17
	Baseline .....	17
	Domus component models and implementation .....	23
3.3	Validation results.....	26
	Cabin in heating mode .....	26
	Cabin in cooling mode.....	26
3.4	Cooling system loop.....	28
3.5	1D physical-based model performance.....	29
4	Efficient model using machine learning (COV).....	32
4.1	Introduction .....	32
4.2	Background.....	32
	Linearity of DEs for thermal systems.....	32
	Supervised machine learning methods .....	33
4.3	Method and materials .....	34
	CWT1 .....	34
	CWT2 .....	35
	CWT3 .....	35
	CWT4 .....	35
	CWT5 .....	35
	Control vector.....	35
	State vector .....	35
	Additional input information.....	36
	Identifying the best model .....	36
4.4	Results .....	37

Model search results .....	37
Evaluation of the best performing model .....	39
4.5 Summary .....	48
5 Performance of the two models (COV/CRF) .....	49
5.1 Comparative performance in terms of accuracy .....	49
5.2 Comparative performance in terms of computational speed .....	49
5.3 Comparative performance in terms of capability .....	49
5.4 Summary .....	50
6 Conclusions (CRF / COV) .....	51
7 Recommendation .....	52
8 Risk register .....	53
9 References .....	54
10 Acknowledgement .....	55
11 Appendix A – Quality Assurance .....	56

## List of Figures

Figure 1. Interaction between work-packages within DOMUS .....	14
Figure 2: Modelling diagram .....	16
Figure 3: Baseline climate system model sketch .....	17
Figure 4: Evaporator left rear section (refrigerant inlet) AMESim model .....	18
Figure 5: Air PTC AMESim model .....	18
Figure 6: Cabin AMESim model in cooling mode. Note that this diagram is provided to give a high-level view of the system and some of the writing may be too small to read. ....	18
Figure 7: Cabin AMESim model in heating mode. Note that this diagram is provided to give a high-level view of the system and some of the writing may be too small to read. ....	19
Figure 8: Compressor AMESim model .....	20
Figure 9: Condenser AMESim model .....	20
Figure 10: Chiller AMESim model .....	21
Figure 11: Example of TXV 4-quadrants diagram.....	21
Figure 12: TXV AMESim model .....	21
Figure 13: Battery (thermal) AMESim model .....	22
Figure 14: PWT AMESim model.....	22
Figure 15: Liquid heater AMESim model .....	22
Figure 16: PWT LT radiator AMESim model .....	23
Figure 17: Coolant pump AMESim model.....	23
Figure 18: Coolant 3-ways valve AMESim model .....	23
Figure 19: Radiant panel AMESim model .....	24
Figure 20: Glazing AMESim model evolution .....	24
Figure 21: Baseline vs. New climate system configuration .....	25
Figure 22: Cabin heater AMESim model.....	25
Figure 23. New HVAC designed by DENSO.....	26
Figure 24: Experimental vs. simulated cabin air temperature in heating mode (cabin calibration model) ..	26
Figure 25: Experimental vs. simulated cabin air temperature in cooling mode (cabin calibration model) ..	27
Figure 26: Experimental vs. simulated vent air temperature in cooling mode (cabin calibration model) ...	27
Figure 27: Experimental vs. simulated air temperature at EVA outlet in cooling mode (climate system calibration model) .....	28
Figure 28: Experimental vs. simulated vent air temperature in cooling mode (climate system calibration model) .....	28
Figure 29: Experimental vs. simulated cabin air temperature in cooling mode (climate system calibration model) .....	28
Figure 30: Experimental vs. simulated 2-phase system HP and LP in cooling mode (climate system calibration model) .....	29
Figure 31: Model accuracy for cabin air temperature evaluation in heating mode.....	30
Figure 32: Model accuracy for cabin air temperature evaluation in cooling mode .....	30
Figure 33: Model accuracy for 2-phase system high pressure evaluation in cooling mode .....	30
Figure 34: Model accuracy for 2-phase system high pressure evaluation in cooling mode .....	31
Figure 35 Example ANN involving 4 inputs, 1 hidden layer with 5 nodes in the hidden layer, and 3 outputs .....	34
Figure 36 Overview of hyper parameter search .....	37
Figure 37 ReLU performs poorly but is helped by dropout whereas other activation functions work better without dropout.....	38
Figure 38 Taking away ReLU and dropout results shows that linear activation is the best performer of the remaining 3 options for final activation .....	38
Figure 39 No significant difference (based on the boxplot) between linear and tanh hidden activation for linear final activation without dropout. Sigmoid is slightly worse whereas ReLU is much worse. ....	39
Figure 40. Comparison of simulation produced curve for sensor 161 versus measurement data from CWT (without smoothing). ....	40
Figure 41. Simulation versus CWT for relative humidity.....	40
Figure 42. Simulation versus CWT for air velocity at driver's head.....	41



Figure 43. ML-simulator correctly and independently tracks driver's head (s161), chest (s163), and foot (s165) temperatures over a 3 hour trial (CWT2) with only small errors. ....	41
Figure 44. Passenger side air temperatures are reasonably accurately tracked with clear differences during the early phase between head (s167), torso (s169), and foot (s171) for trial CWT1.....	42
Figure 45. Comparison for CWT trial 3 Sensor 161 (driver head air temperature).....	42
Figure 46. Comparison for CWT trial 3 Sensor 39 (windshield temperature driver's side) .....	43
Figure 47. CWT-1 simulated versus measurement for driver head temperature and HCM comfort score. The HCM score is converted to an integer and multiplied by 10 to show on the same axis. Note that the simulated estimate lags the true value of the cabin temperatures and this is reflected by a lag in the simulated HCM score. ....	45
Figure 48. CWT-2 simulated versus measurement for driver head temperature and HCM comfort score. Around the 1000 s mark, the temperatures come close to the HCM's threshold causing the HCM to oscillate rapidly between comfortable and uncomfortable. This is partly due to noise in the sensor measurement. The simulated values are smoothed and thus do not see such oscillation.....	45
Figure 49. CWT-1 HCM confusion matrix between the HCM based on measurement (or "true" labels) versus the HCM based on simulated measurement (termed "predicted"). Only 1.3% total are misclassified. ....	46
Figure 50. CWT-2 HCM confusion matrix. In this case, 3.4% are misclassified. ....	46
Figure 51. CWT-3 HCM confusion matrix. In this case, 2.5% are misclassified. ....	47

## List of Tables

Table 1 Summary of neural network activation functions .....	33
Table 2 Top 10 results from hyper parameter search showing that best performer is a linear network with no hidden layers .....	39
Table 3. Performance of machine-learnt simulator in terms of error for each sensor. Average air temperature (avg_air) is based on comparing the average of head, torso and foot air temperatures for driver and front passenger with that of the simulated values. The table is sorted by NRMSE.....	44

## Abbreviations

Symbol / Shortname	
<b>AC</b>	Air Conditioning
<b>AMESim</b>	AMESim simulation software
<b>ANN</b>	Artificial Neural Network
<b>BEV</b>	Battery Electric Vehicle
<b>CAD3D</b>	Virtual geometrical model of the part
<b>CAN</b>	Controller Area Network (bus)
<b>CD</b>	Cool-down protocol
<b>CFD</b>	Computational Fluid Dynamics
<b>CO2</b>	Carbon dioxide
<b>CWT</b>	Climatic Wind Tunnel
<b>DE</b>	Differential Equation
<b>EDM</b>	Electric Drive Module
<b>eps-NTU</b>	Number of Transfer Units (NTU Method)
<b>EVA</b>	Evaporator
<b>GTSuite</b>	GTSuite simulation software
<b>HP</b>	High Pressure
<b>HVAC</b>	Heating, Ventilation, Air Conditioning unit
<b>HX</b>	Heat Exchanger
<b>LP</b>	Low Pressure
<b>LR</b>	Linear Regression (or alternatively Multivariate Linear Regression)
<b>LT</b>	Low Temperature Radiator
<b>MSE</b>	Mean Squared Error
<b>NARX</b>	Non-linear autoregressive systems with exogenous inputs
<b>NRMSE</b>	Normalised RMSE
<b>PCM</b>	Phase Change Material
<b>PTC</b>	Positive Temperature Coefficient electric heater
<b>PVB</b>	Polyvinyl butyral
<b>PWT</b>	Power Train
<b>ReLU</b>	Rectified linear unit
<b>RMSE</b>	Root Mean Squared Error
<b>RT</b>	Real Time factor or time to compute 1 second of simulation
<b>TES</b>	Thermal Energy Storage
<b>TXV</b>	Thermal Expansion Valve
<b>WU</b>	Warm-up protocol

# 1 Purpose of the document

## 1.1 Document structure

The document is divided into sections that provide:

- an introduction and description of common methodological elements
- description of the 1D simulator and associated results
- description of the ML simulator and associated results
- comparison of the two simulators
- recommendations

## 1.2 Deviations from the original description in the Grant Agreement Annex 1- Part A

### Description of work related to deliverable in GA Annex 1 – Part A

The high-level description of task 1.4 is as follows:

Develop an efficient, low-fidelity model of the car cabin thermal and acoustic environment. Measure: The models should be within 5% accuracy of the high-fidelity model for outputs such as temperature and holistic comfort should be with an accuracy of 10%.

The more detailed description is:

Task 1.4 Efficient cabin / comfort model (COV, CRF, ika, ViF) M12 – M28

Task 1.4 aims to produce a highly efficient, low-fidelity 1D model of the thermal environment within the car cabin. In addition, a separate acoustic model will also be developed. The 3D model of the car cabin is used as input to this task. The 1D model will attempt to approximate a small subset of the outputs of the 3D model to directly, or indirectly identify the thermal cabin comfort over time. This 1D model is based on the observation that a large and complex set of differential equations can sometimes be approximated by a smaller set of differential equations. Two approaches are taken to developing the model to reduce risk. The first approach (led by CRF) starts with a sophisticated thermal model that accounts for all contributions to the heat exchange between the cabin and the surrounding environment, including interior components such as dashboard, internal trims, and seats. Successive simplifications reduce this model to one that can be efficiently computed but which remains reasonably accurate. Similarly, a model of NVH will be derived and simplified. The second approach (led by COV) uses dynamical data from physical and / or 3D experiments to derive a dynamic thermal model of the car cabin. A machine learning algorithm, such as artificial neural networks, might be used to derive this mapping. Similarly, a machine-learned model of the NVH will be derived from the 3D NVH model and / or experimental data. The efficient cabin model will be validated both in terms of specific outputs, such as temperature at the headrest, and overall holistic comfort, using the holistic comfort model and experimental data produced in T1.2. The most effective approaches will be selected as an output and used in other work packages. Inputs: D1.2, D1.3 Outputs: D1.4 (Used by WP2 (T2.3) and WP6)

Partner contributions

COV: task leader, development of 1D thermal and NVH models from experimental and 3D model data using machine learning

ika: production a requisite data base with the 3D model from Task 1.3 for supporting the generic 1D model development. ViF: Integrate highly efficient, low-fidelity 1D model of the acoustic environment within the car cabin with holistic comfort model and provide validation

CRF: perform the development of analytical 1D thermal and NVH models.

The models should be within 5% accuracy of the high-fidelity model for outputs such as temperature and holistic comfort should be with an accuracy of 10% and meets simulation requirements of WP2.

#### Time deviations from original planning in GA Annex 1 – Part A

The initial delivery for this task was estimated at M28 based on the completion of work on the CFD models to be completed on-time at M24. The CFD models, however, were delayed by late arrival of the validation data for the car cabin. This work was therefore rescheduled for M30 to coincide with the delivery of D1.4, which was also rescheduled to this date. Further delays in the arrival of the validation data meant that D1.4 was further delayed and at this stage, the dependence on data from D1.4 was relaxed and data produced in Climatic Wind Tunnels by CRF were used instead.

Note that the late arrival of the validation data for the car cabin was caused by the late access of FCA as fully flagged partner in the project, following the first amendment of the project, the process for which was completed at the end of the first project year. Moreover an unforeseen extensive NVH testing campaign was to be carried out first, for the sake of the acoustic modelling by Power Injection Method.

The revised schedule for D1.5 is to provide a draft at M30 for review and finalisation by M31.

#### Content deviations from original planning in GA Annex 1 – Part A

As noted above, the basis for this work is the CFD model results from D1.4, which have not been provided in time. A revised approach is to use the CWT results for the machine-learned simulator. This limits the applicability of the final ML simulation since it is not possible to incorporate optional components such as radiant panels. Therefore, it is still desirable to revise the ML simulation once D1.4 results are fully available.

Furthermore, the acoustic or NVH model is now being described in D1.4.

## 2 Introduction (COV/CRF)

### 2.1 Objectives

The aim of this deliverable is to produce an efficient (meaning, fast to compute) simulation of the thermal environment of the cabin. In contrast to the grant agreement, it was decided to include the acoustic simulation work only in deliverable D1.4, as the acoustic simulation given there is already sufficiently efficient.

The main outputs of this deliverable are:

1. A description of the methods used to obtain the two simulators.
2. A 1D simulation that is capable of simulating the HVAC internal operation, the thermal environment within the cabin in simplified form, and various DOMUS components, such as radiant panels.
3. A Machine Learnt (ML) simulation that is capable of simulating the thermal environment in greater detail (than the 1D simulator) and is much faster but does not simulate the HVAC internals or the DOMUS components.

The measures established in the grant agreement for this deliverable require the following targets to be met:

1. The models should be within 5% accuracy of the high-fidelity model for outputs such as temperature and,
2. Holistic comfort should be estimated with an accuracy of 10%.

For the purposes of this deliverable, we take these accuracy requirements to be based on the normalized root mean square error (NRMSE) as described in Section 2.4.

### 2.2 Relationship to DOMUS objectives

DOMUS project aims to reduce energy consumption of electric vehicles (e.g., minimize consumption of components, reduce losses, remove unnecessary consumptions). The car cabin's heating and cooling system is the car's largest auxiliary load, however this system is closely related to personal comfort (critical to customer satisfaction) and some of this functionality is needed for safety (e.g., defogging the windscreen).

The overall aim of WP1 is to provide an efficient virtual method for the user-centric assessment of the energy use of a car cabin and climate control system while ensuring it meets expectations for comfort and safety (see Deliverable D1.3).

This overall aim is broken into objectives of providing a framework for assessment, including a fitness function (Task 1.1, Deliverable D1.2), a method of estimating holistic comfort of passengers given information about their thermal and acoustic environment (Task 1.2, Deliverable D1.3), a high fidelity (or slow) model of the thermal and acoustic environment (Task 1.4, Deliverable D1.4), and a low fidelity (or fast) model of the thermal and acoustic environment (this deliverable). Note that it was decided to only include one model of the acoustic environment as this model is already sufficiently fast. That model is provided in Deliverable 1.4.

Within WP1, Task 1.4 (this deliverable) aims to provide a computationally fast simulation model of the thermal environment within the cabin.

### 2.3 Relationship to other work packages and tasks

As shown in Figure 1 below, WP1 has various flows of information to and from other work packages. With regard to this task, the relevant flow is to provide a generic cabin model to WP2. Also, WP5 makes use of the cabin model to help develop an optimised control logic to control the HVAC.

Note that T1.3 (Deliverable D1.4) already aims to provide a 3D CFD cabin model. This model, while accurate, is computationally slow. For WP2 and WP5, a much faster simulation model is required. Specifically,

- WP2.3 requires fast simulation to support machine learning of cabin configurations.
- WP5.1.2 requires fast simulation to support machine learning of cabin control logic.

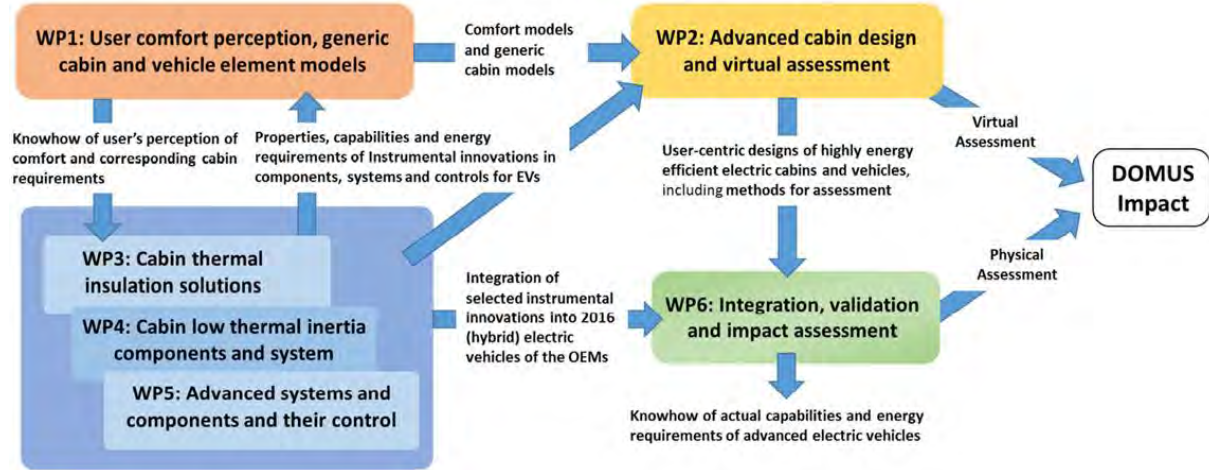


Figure 1. Interaction between work-packages within DOMUS

## 2.4 Methodology common to both approaches

The DOMUS grant agreement mentions specific measures for the deliverables and results for each task. For example, the T1.4 model aims to have an accuracy that is within 5% of the high-fidelity model in terms of temperature. However, a key question then becomes how to calculate the percentage error correctly. If the values are given in kelvin, this might yield a different result than if in degrees Celsius, for example. Furthermore, simulation may tend to diverge or converge over time and thus average error after 1 second of simulation may be quite different from the error after 1 minute of simulation. This document aims to set out a way of consistently reporting error so that results from different groups can be fairly compared.

### Error reporting

Given some set of  $N$  measurements  $X = x_1, x_2, \dots$  and some estimate of those values  $\hat{X} = \hat{x}_1, \hat{x}_2, \dots$ , the mean squared error is:

$$MSE_{X, \hat{X}} = \frac{1}{N} \sum_i (x_i - \hat{x}_i)^2$$

The root mean squared error is

$$RMSE_{X, \hat{X}} = \sqrt{MSE_{X, \hat{X}}}$$

The normalised RMSE or percentage error is the error in terms of the possible range of values

$$NRMSE_{X, \hat{X}} = \frac{RMSE_{X, \hat{X}}}{x_{\max} - x_{\min}} \cdot \frac{100}{1} \%$$

Errors or uncertainties should be accompanied by details of the forecast period. For example, a simulation begins with the same initial conditions as a climatic wind tunnel test and is run for a certain simulated duration, such as 20 minutes. This duration will affect the error estimate.

One approach might be to fix the simulation duration to 10 minutes. An alternative approach, and the one taken here, is to first graph the results and check for any increasing divergence over time. Where divergence occurs, this can be separately reported. If no divergence occurs, the NRMSE value can be applied to the whole simulation period.

Several simulation run results may be combined by aggregating into a single large  $X$  set prior to calculating the RMSE.

The sample periodicity of the underlying simulation can safely be ignored as long as it is a fixed period. A simulation that produces estimates every second can reasonably be compared to a simulation that produces estimates every 10 seconds, for example. If, however, more samples are produced at some time points in the simulation, resampling is needed to ensure that the period is fixed and that all parts of the simulation are weighted equally.

### 3 Efficient 1D model using traditional methods (CRF)

#### 3.1 Methods for obtaining the model

To model the North America 500 BEV climate system AMESim software, version 17.0, has been used: it is a programming environment developed for the object-oriented modelling of complex physical systems. The main used libraries are: thermal, thermo-hydraulic, two-phase flow, heat, air-conditioning.

The heating mode and the cooling mode have different airflow distribution, tri-level and only vent respectively. The airflow distribution has effect on the heat exchange coefficient on the cabin wall. Due to this phenomenon, two different models, one for heating and one for cooling operation are set up.

The modelling has been carried out using a bottom up approach: starting from the basic components modelling, the different subsystems have been assembled and then connected to each other until reaching the final system configuration.

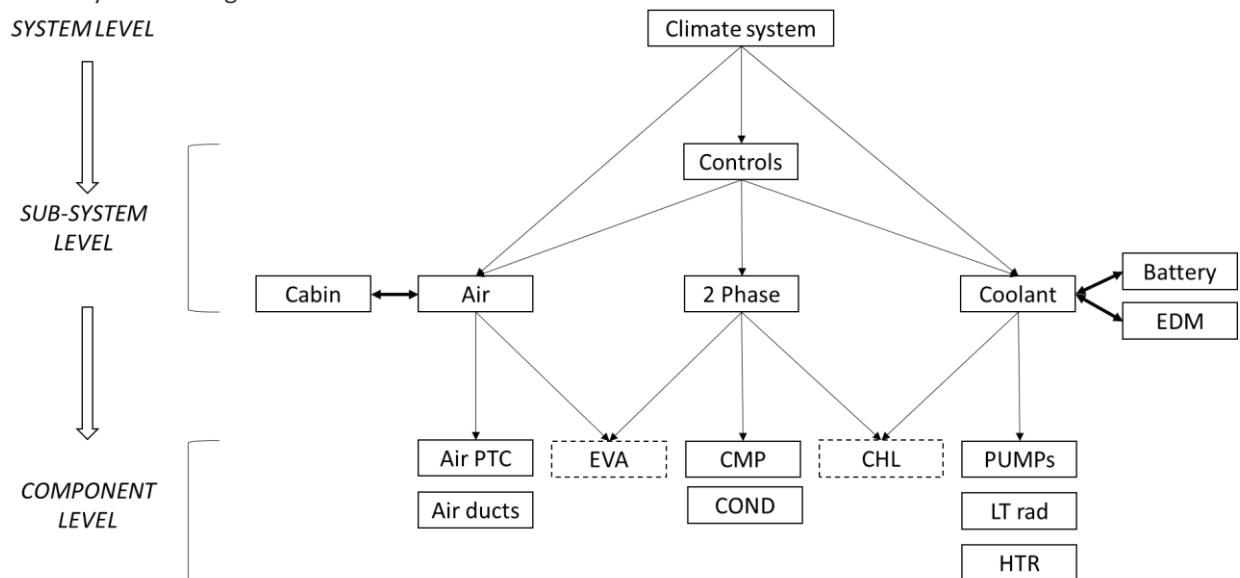


Figure 2: Modelling diagram

Each component has been characterized starting from the available datasheets: the AMESim model from the library of interest has been filled with geometrical and operation data and then calibrated to more accurately fit the performance and pressure drop curves by test bench.

For the cabin a 1D model has been developed, consisting of several thermal masses corresponding to the main inertial masses that interact between them by conduction and radiation and with the air by convection. Geometrical and material data come from A2Mac1 (a platform that harvests and stores the benchmarking information for many OMEs and component suppliers) and CAD3D. The heat exchange parameters have been assumed. The model has been calibrated, in heating and cooling mode, with the experimental data.



## 3.2 Model description

### Baseline

The following sketch shows the current climate system configuration of the 500 e, that is the baseline for DOMUS project:

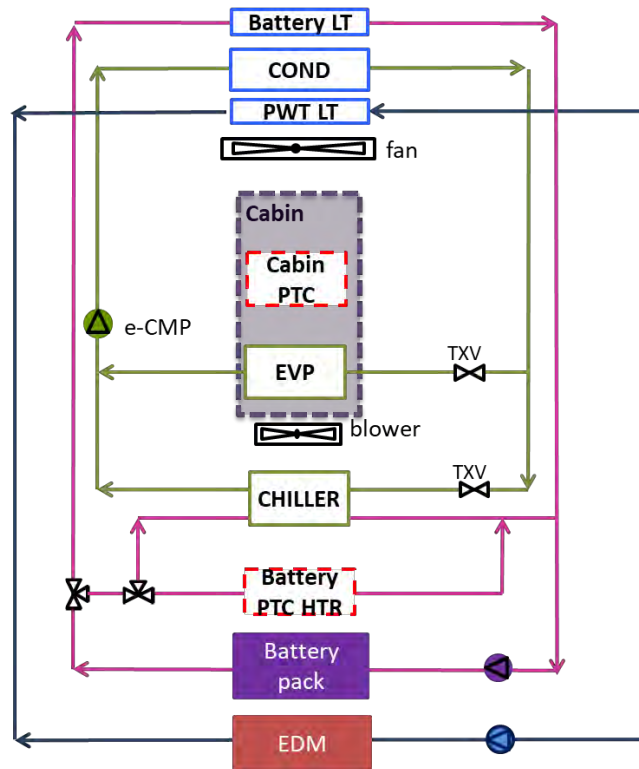


Figure 3: Baseline climate system model sketch

The sketch includes the following sections:

- HVAC system
- Two-phase flow loop (green line)
- Battery (purple line) and PWT (blue line) coolant loops

In the next section each component is described in detail.

#### 3.2.1.1 HVAC

The sub-system includes the evaporator, the air ducts and the air PTC and it is connected to the cabin.

The model has been developed under the following assumptions:

- Blower is modelled as an air source at fixed volume flow rate
- At fixed flow rate, air properties at evaporator inlet depend on the flow source (in partial recirculation mode the air properties result from the mixing of cabin air and external air)
- Air ducts geometry, location and pressure drops are not modelled but only air distribution indications and thermal interactions with the surrounding are taken into account;

##### 3.2.1.1.1 Evaporator

The evaporator is realised with the “tube and fin” technology, with two ranks and 29 tubes per rank. The overall dimensions are  $221 \times 199 \times 38 \text{ mm}^3$ . No AMESim predefined sub-model has been used but an ad hoc model has been developed: the component has been divided in 16 sub-volumes and each sub-volume has been modelled as a refrigerant-aluminium-air thermal series. The sub-volumes interact between them in the following way:

- Refrigerant tubes are connected in series to model the refrigerant flow (one inlet, one outlet)
- Aluminium masses are connected with surrounding masses through conductive heat exchanges

- Front air volumes interact with rear air volumes to model the air flow (one inlet, split of left and right flows on front side, mix of left and right flows on rear side, one outlet).

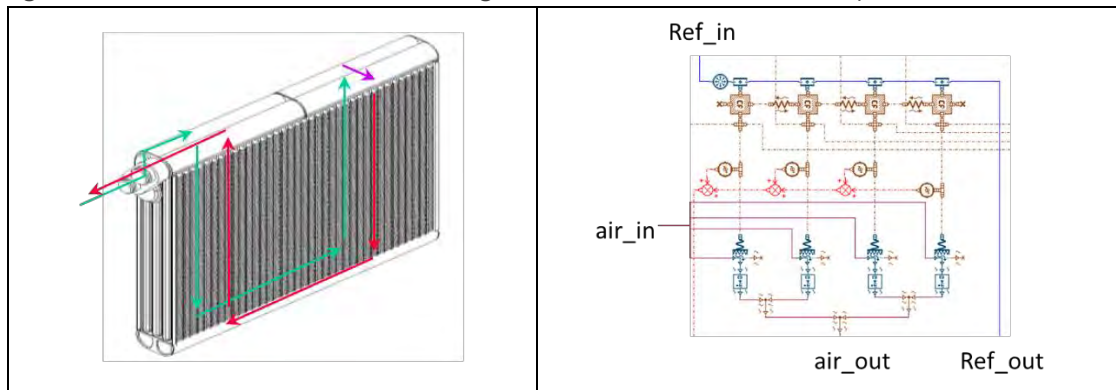


Figure 4: Evaporator left rear section (refrigerant inlet) AMESim model

The component is calibrated to fit the performance (a, b, and c coefficient to  $Nu = a * Re^b * Pr^c$  calculation) and pressure drop coming from the real component datasheet.

#### 3.2.1.1.2 Air PTC

The Cabin PTC is a high-voltage PTC with maximum installed power of 6 kW. In AMESim, it is modelled as an aluminium mass, with an internal heat generation (based on maps depending on air temperature and mass flow rate), thermally connected to an air volume:

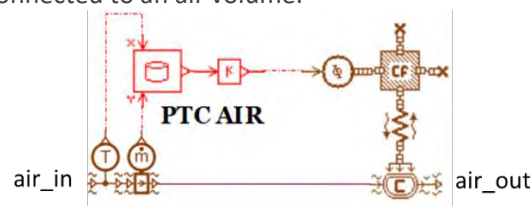


Figure 5: Air PTC AMESim model

#### 3.2.1.1.3 Cabin

Two cabin models are provided due to air distribution changing as function of the operating mode:

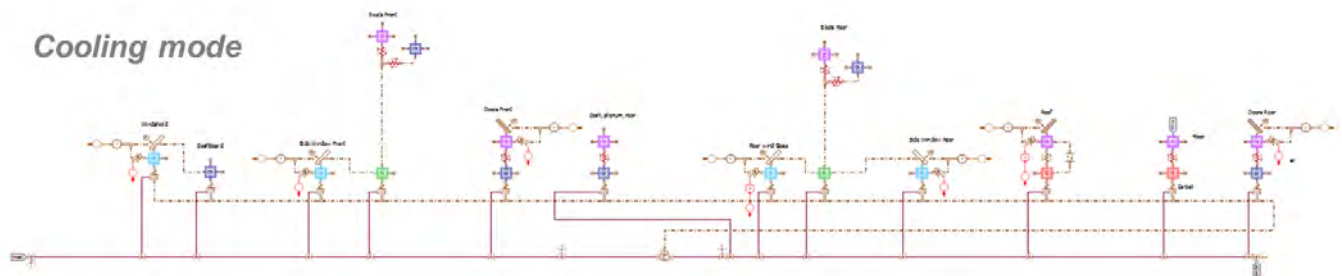


Figure 6: Cabin AMESim model in cooling mode. Note that this diagram is provided to give a high-level view of the system and some of the writing may be too small to read.

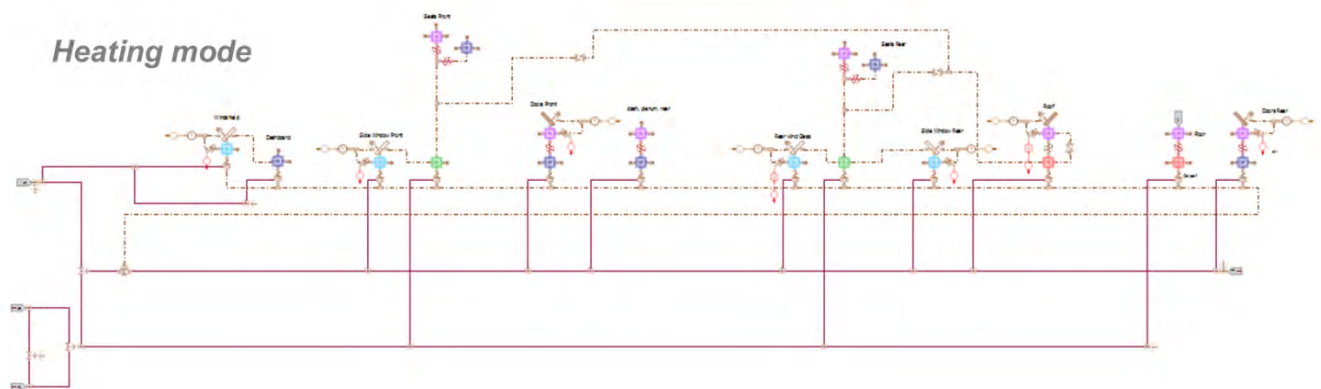


Figure 7. Cabin AMESim model in heating mode. Note that this diagram is provided to give a high-level view of the system and some of the writing may be too small to read.

The cabin model consists of:

- thermal masses, representative of the several materials inside the cabin
- heat exchange: conductive between the thermal masses, convective between the masses and the air, radiative between the faced surfaces and coming from the sun.
- air volume: the inner air is modelled as a unique volume, that thermally exchanges with the cabin inner components and the incoming air (from vent in cooling mode, from floor and defrost in heating mode).

The 2 models have been calibrated using the experimental data from CD test (cooling mode) and WU test (heating mode).

For the calibration only the first 30 minutes of CD and the first 21 minutes of WU tests have been considered: the thermal conductance between the materials in contact and the boundary layer thickness for convection exchanges between materials and air have been manually changed to obtain the combination that returns a simulated cabin air temperature as close as possible to the experimental trend, calculated as average of air temperatures for head, feet and body zones.

Since a single air volume is assumed, the air distribution is taken into account in the number of incoming air ports:

- In cabin cooling, a single air flow is representative of the vent distribution
- In cabin heating, 3 air flows model front floor, rear floor and defrost inlets

Left and right sides are not differentiated, front and rear components location is taken into account in thermal connections between incoming air flows and materials:

- In cabin cooling, the air flow comes from front side inlets, so it firstly interacts with the front components (air conditions as in inlet) then with the rear components (air conditions after the thermal exchange)
- In cabin heating the air flow from the defroster partially interacts with the windshield and the dashboard, the air flow from feet inlets partially interacts with the seats and the floor and the remaining flow has heat exchange with the upper interior components.

### 3.2.1.2 Two-phase flow loop

The two-phase flow system includes the compressor, the heat exchangers and the valves.

#### 3.2.1.2.1 Compressor

An electrical compressor with fixed displacement of  $33 \text{ cm}^3$  is used. The component has been modelled with the AMESim predefined sub-model, based on volumetric, isenthalpic and mechanical efficiency maps as function of pressure ratio and compressor speed to calculate the mass flow rate and enthalpy variation. The compressor speed is controlled inside the range  $[1000, 8600]$  rpm to reach the target air temperature at evaporator outlet.

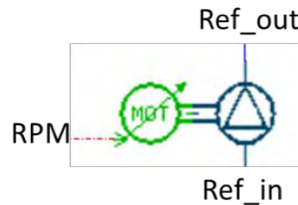


Figure 8: Compressor AMESim model

#### 3.2.1.2.2 Condenser

The air condenser is a  $620 \times 313 \times 16 \text{ mm}^3$  heat exchanger, with 4 passages including sub-cooling section, 35 tubes and an integrated receiver. It is modelled with the predefined AMESim sub-model that is characterized with the geometry and position specifications, the flow configuration and the internal pressure drop coefficient. The model supports the "HEAT stack" tool to simulate the thermal interactions with front-end HXs.

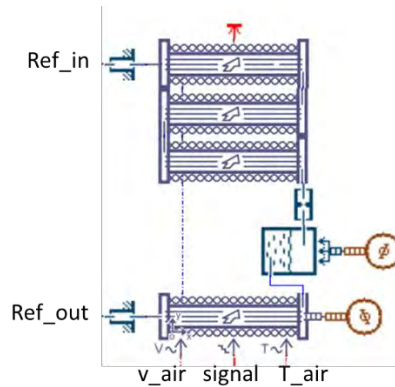


Figure 9: Condenser AMESim model

The component is calibrated to fit the performance (a, b, and c coefficient to  $Nu = a * Re^b * Pr^c$  calculation) and pressure drop coming from real component datasheet.

### 3.2.1.2.3 Chiller

The chiller is a 15 plates heat exchanger, 3 ranks and "I" flow configuration, for which an ad hoc model has been built up as for the evaporator. The refrigerant and coolant flows are respectively split in 3 parallel branches, one for rank, and for each branch 2 sub-volumes are modelled. Each sub-volume, representative of a 1/6 of chiller, is modelled as a refrigerant-aluminium-coolant thermal series and is connected to the others according to the flow configuration. The component is manually calibrated to fit the experimental performance (a, b, and c coefficient to  $Nu = a * Re^b * Pr^c$  calculation) and pressure drop.

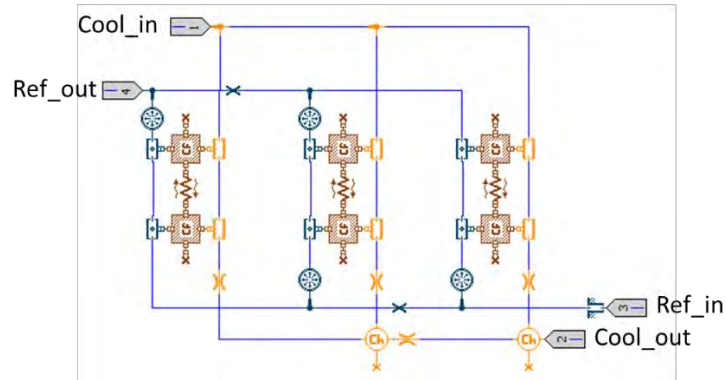


Figure 10: Chiller AMESim model

### 3.2.1.2.4 Valves

Lamination valves are TXVs of 1.5 ton (about 5.3 kW of cooling power), equal for chiller and evaporator. The valve modelling is obtained using the predefined AMESim sub-model, based on 4-quadrant characterization

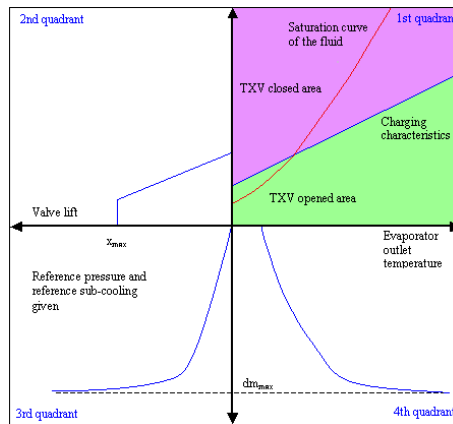


Figure 11: Example of TXV 4-quadrants diagram

The component operates to regulate the superheat at the evaporator/chiller outlet:



Figure 12: TXV AMESim model

### 3.2.1.3 Coolant loop

The coolant loop provides battery and PWT thermal management.

#### 3.2.1.3.1 Battery pack

The battery pack consists of 96 prismatic cells of 60 Ah/cell, for a total pack energy of 22 kWh. The model reproduces the pack stratification (case, cells, cooling plate) as a series of thermal masses of different materials thermally connected between them by conductive heat exchanges and connected to the coolant flow by convective heat exchange. The pressure drop is given as a function of liquid flow rate,

defined inside a resistive component (i.e. valve). The pack model has a vertical orientation, so the upper side interacts with the cabin and the lower side with the ambient

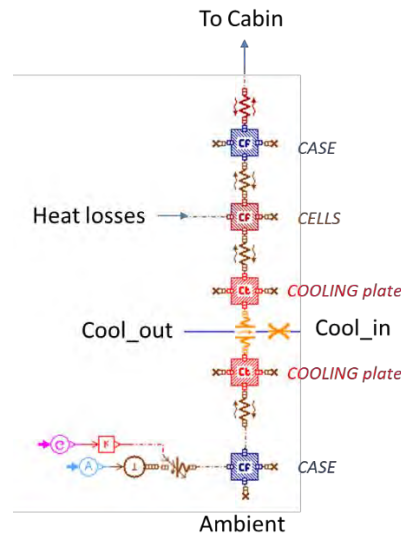


Figure 13: Battery (thermal) AMESim model

#### 3.2.1.3.2 PWT

The PWT consists of electric machines, charger and inverter. For the scope of the modelling these components are seen as waste heat sources on coolant loop, so modelled as an aluminium mass, with an internal heat generation, thermally connected to a liquid pipe. The pressure drop is introduced by a resistive component, generally a valve (orifice diameter or pressure drop curve), in series to the thermal sub-model. A two sub-volumes discretisation is used for a more accurate modelling:

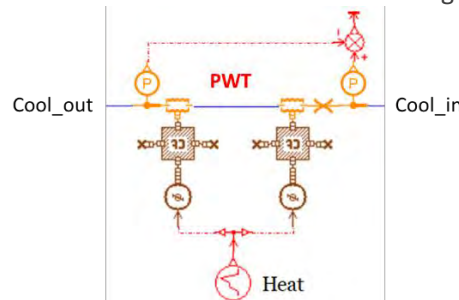


Figure 14: PWT AMESim model

#### 3.2.1.3.3 Liquid Heater

The liquid heater is a 5 kW electrical heater, modelled as an aluminium mass, with an internal heat generation (based on maps depending on air temperature and mass flow rate), and thermally connected to a liquid pipe with friction modelling. A two sub-volumes discretisation is used to obtain a more accurate modelling:

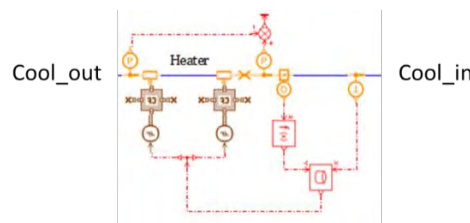


Figure 15: Liquid heater AMESim model

#### 3.2.1.3.4 PWT LT radiator

The PWT radiator is a  $620 \times 390 \times 18 \text{ mm}^3$  heat exchanger, modelled using the predefined AMESim sub-model for liquid-gas cross flow HXs. The model requires the overall, internal and external geometry, position

specifications, the flow configuration and the internal pressure drop definition; a specific tool, based on eps-NTU method, is used for the heat exchange calibration with performance curves from datasheet. The model supports the “HEAT stack” tool to simulate the thermal interactions with front-end HXs.

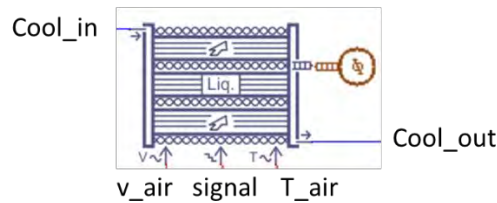


Figure 16: PWT LT radiator AMESim model

#### 3.2.1.3.5 Battery LT radiator

The battery pack radiator is a  $610 \times 143 \times 21 \text{ mm}^3$  heat exchanger, modelled using the predefined AMESim sub-model for liquid-gas cross flow HXs, also used for PE LT radiator modelling.

#### 3.2.1.3.6 Fan

The fan contribution to the operation is introduced through the air velocity maps as function of vehicle velocity and high pressure of the refrigerant loop, supplied in input to the front-end module.

#### 3.2.1.3.7 Pumps

A 50W pump on the PWT loop and a 100W pump on the battery loop are used. The component is modelled with the AMESim sub-model, provided in thermal hydraulic library

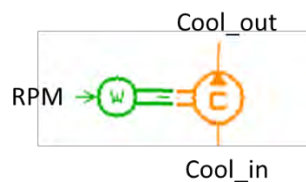


Figure 17: Coolant pump AMESim model

The component behaviour is deduced by the pressure increase map as function of coolant volumetric flow rate and pump speed.

#### 3.2.1.3.8 3-ways valve

To model this component the predefined AMESim model is used

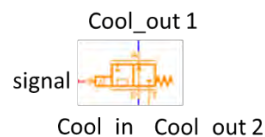


Figure 18: Coolant 3-ways valve AMESim model

Each valve port has a name to identify it: A, P and T. Each path is indicated by the two letter one for the inlet and one for the outlet. The PA and PT paths are enabled (AT is always OFF) and the path opening depends of input signal (for each path a mathematical equation, function of the input signal, define the passage cross section area). The flow can be managed in each path at the same time.

### Domus component models and implementation

The cabin has been modified and the following contents added:

- Radiant panels
- Glazing
- Insulation panels with PCM
- Heated seats

In addition, the system model has been modified with the introduction of the thermal storage on coolant loop with the cabin heater and a bi-level HVAC.



#### 3.2.1.4 Radiant panels

They are provided on all surfaces except glazing and roof for a total installed power equal to 2000 W. Each panel is able to release a maximum radiative power that could be tuned on a setting temperature. At model level, an additional mass, with an internal heat generation depending on a temperature target, has been thermally connected (radiative heat exchange) to the surface of interaction.

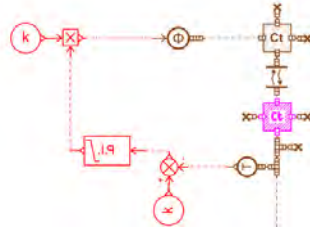


Figure 19: Radiant panel AMESim model

#### 3.2.1.5 Glazing

All transparent surfaces are involved.

At equal surface area, a three-layer glazing is introduced for all the surfaces (glass + PVB + glass), not only for windshield, and the optical parameters of the outer glass change influencing the heat exchanges with the external environment.

At model level the thermal mass, representative of the single glass layer, is substituting with a thermal wall with 3 different material layers.



Figure 20: Glazing AMESim model evolution

#### 3.2.1.6 Insulation panels

On the roof, doors and dashboard, the insulation panels are installed to thermally insulate the cabin from the external environment. A phase change material (PCM) layer with melting temperature of 15°C is introduced. This layer operates as additional heat capacity to the cabin (heat source in cabin heating and heat sink in cabin cooling).

At model level a thermal mass has been added to the stratigraphy of the cabin panels for which the insulation is provided (thermal connection with conductive heat exchange).

#### 3.2.1.7 Heated seats

Faurecia heated and ventilated seats are added to the cabin interior: seats are provided with heated mats on cushion and backrest, integrated in the seats, in addition to the radiant panel on the rear side of the backrest (only for front seats). Ventilated seats are not simulated.

At model level an additional thermal mass, with an internal heat generation depending on a temperature target, has been thermally connected (radiative heat exchange) to each surface of interest (equal to radiant panels).



### 3.2.1.8 Coolant loop

The coolant sketch has been modified as follows:

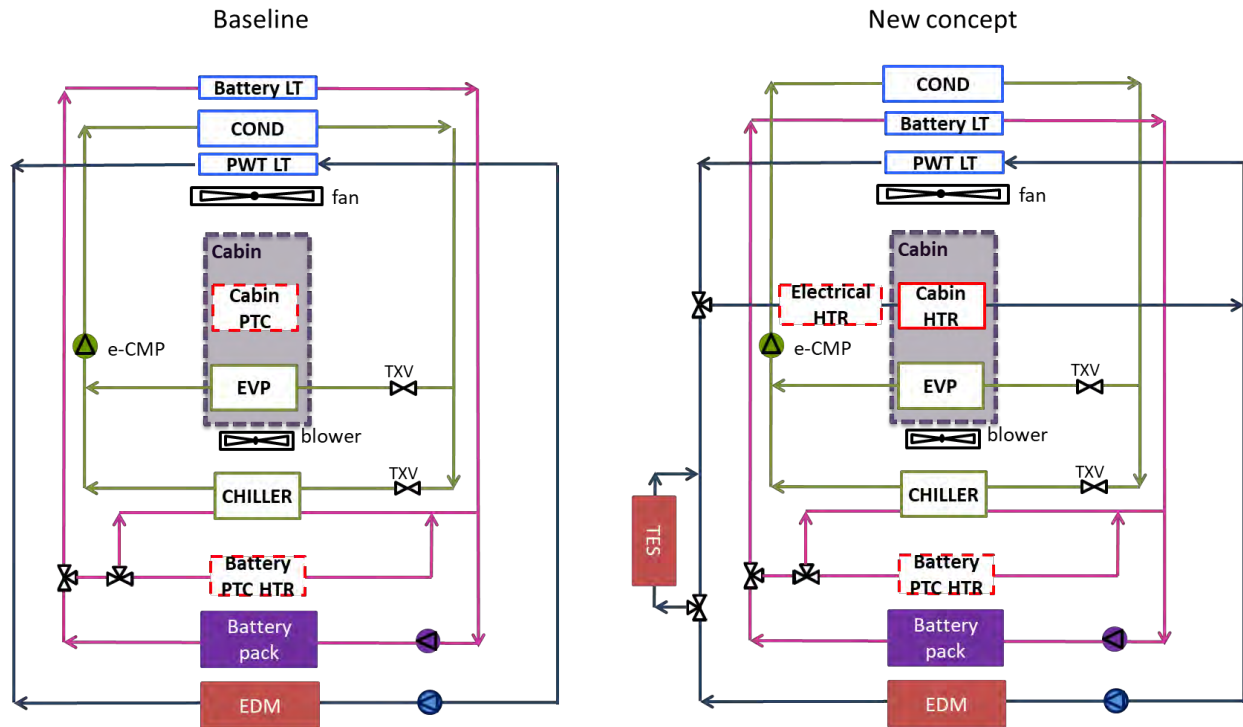


Figure 21: Baseline vs. New climate system configuration

On PWT loop (blue line) the following components have been added: a TES to store waste heat from EDM, a cabin heater to release the waste heat to cabin when the cabin heating is required and two 3-ways valves. The cabin PTC inside the HVAC has been substituted with an electric heater upstream the cabin heater. The HXs location on front-end module has been modified.

The electrical heater has been modelled as the battery liquid heater and the 3-ways valves on PWT loop as the coolant valves on the battery loop (see previous paragraph). The cabin heater has been modelled using the predefined AMESim model that support a calculation tool to define the overall heat transfer coefficient using the eps-NTU method starting from experimental data. The pressure drop on coolant side is given by adding a resistive component, i.e. a valve:



Figure 22: Cabin heater AMESim model

### 3.2.1.9 Re-designed HVAC

The re-designed HVAC provides a different air distribution respect to the standard production. The detailed description of the system has been carried out in Deliverable D5.3.

From the simulation point of view, the re-designed HVAC modelling traduces in the air flow rate variation at the cabin inlet port.

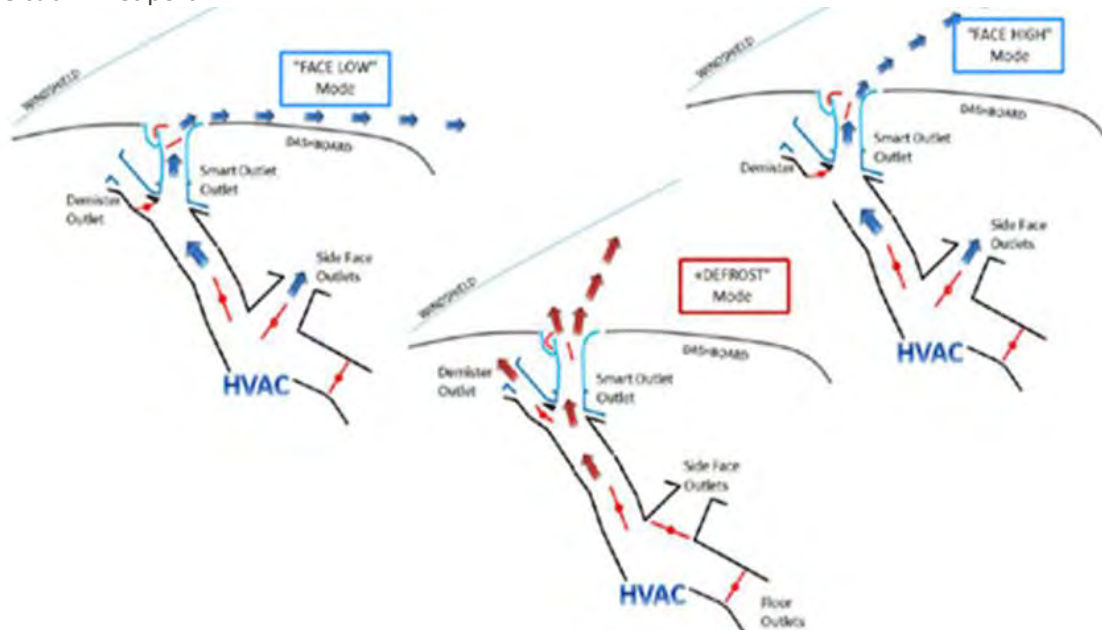


Figure 23. New HVAC designed by DENSO

## 3.3 Validation results

### Cabin in heating mode

The heating cabin model has been validated on first phase (21 minutes) of the FCA standardized WU test. The validation data coming from measurement performed by CRF in the FCA wind tunnel facility. The validation model includes the air ducts, the cabin and the cabin PTC. The air flow entering into the HVAC comes from the external environment (recirculation OFF).

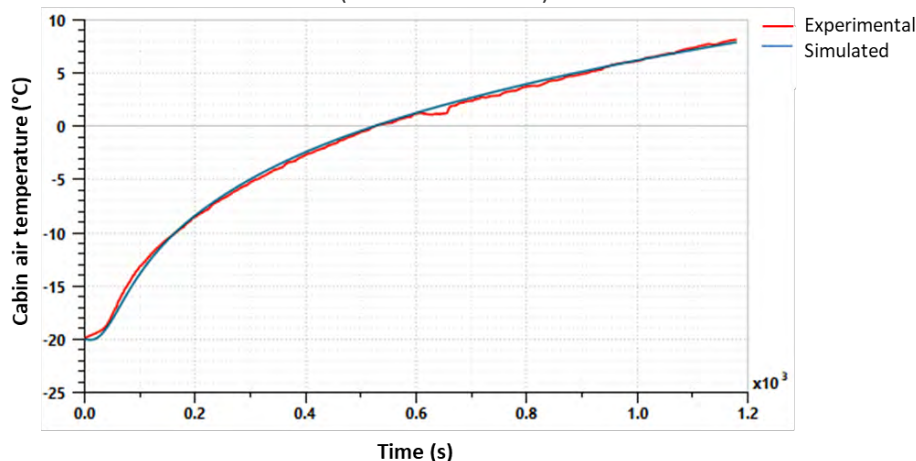


Figure 24: Experimental vs. simulated cabin air temperature in heating mode (cabin calibration model)

The simulated average cabin temperature fits the experimental value well (RMSE=0.1K), calculated as mean value of air temperature at front and rear head, body and feet zones.

### Cabin in cooling mode

The cooling cabin model has been validated on first phase (30 minutes) of the FCA standardized CD test. The validation model includes the air ducts and the cabin; the properties of the air flow coming from the

evaporator are the model inputs (experimental data). The following pictures show the comparison between the simulated and experimental temperatures trend.

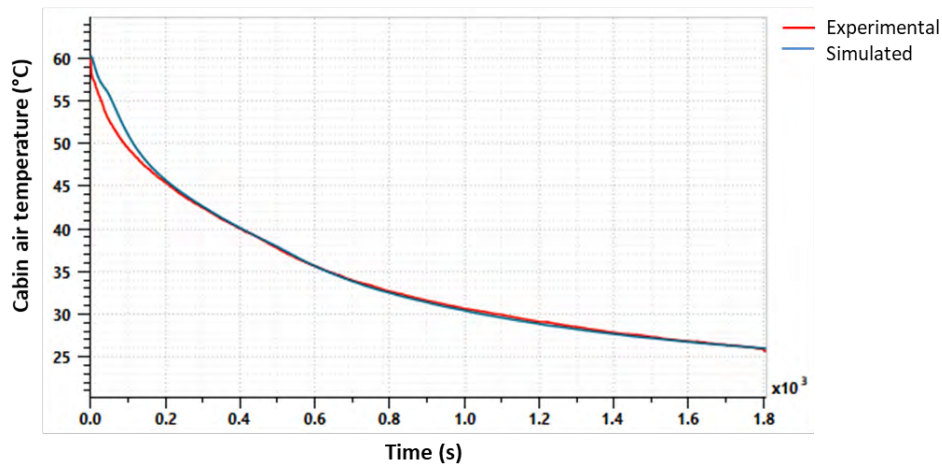


Figure 25: Experimental vs. simulated cabin air temperature in cooling mode (cabin calibration model)

The average temperature of cabin air fits the experimental one well (RMSE=0.1K) in the first phase.

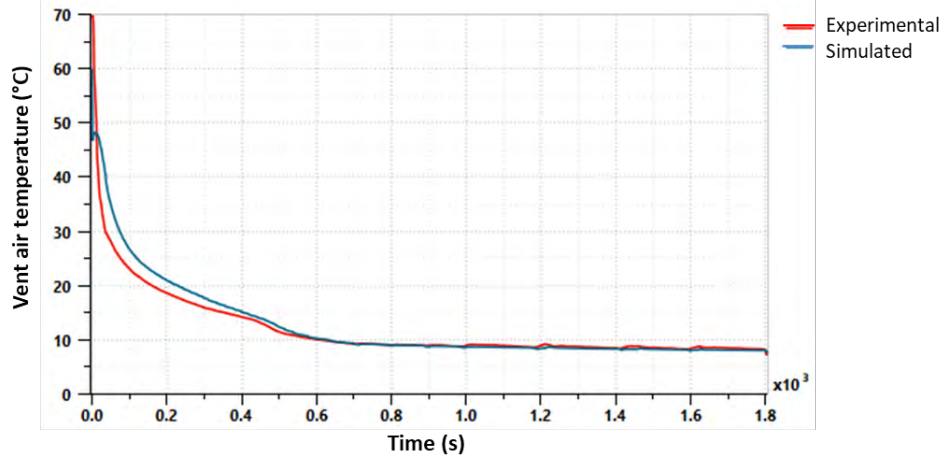


Figure 26: Experimental vs. simulated vent air temperature in cooling mode (cabin calibration model)

The vent temperature fits the experimental trend well (RMSE=0.2K) during all the phases in recirculation.

### 3.4 Cooling system loop

The assembled model has been validated on the experimental data. For the heating mode, the cabin calibration model corresponds to the cabin climate model. For the cooling mode, the model has been validated of the first CD test phase (30 minutes) due to the limitation of the AMESim software for the zero-flow modelling (when the second phase starts the chiller is closed and the battery is cooled down by LT radiator).

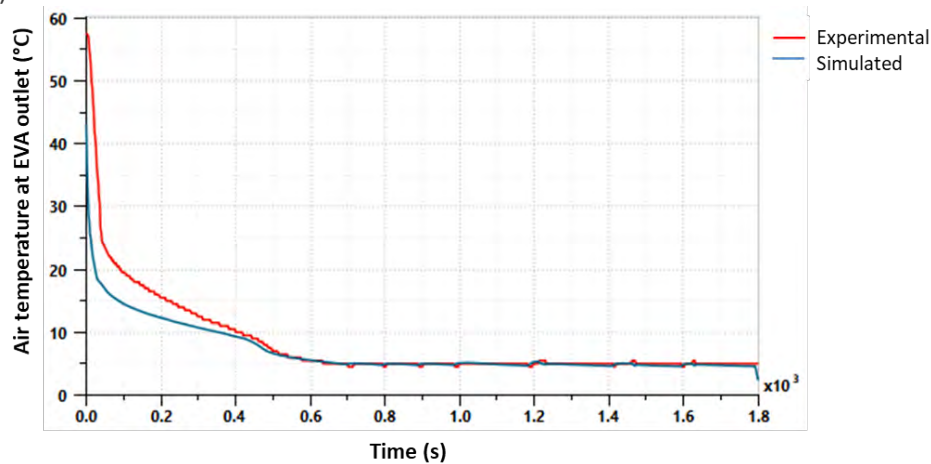


Figure 27: Experimental vs. simulated air temperature at EVA outlet in cooling mode (climate system calibration model)

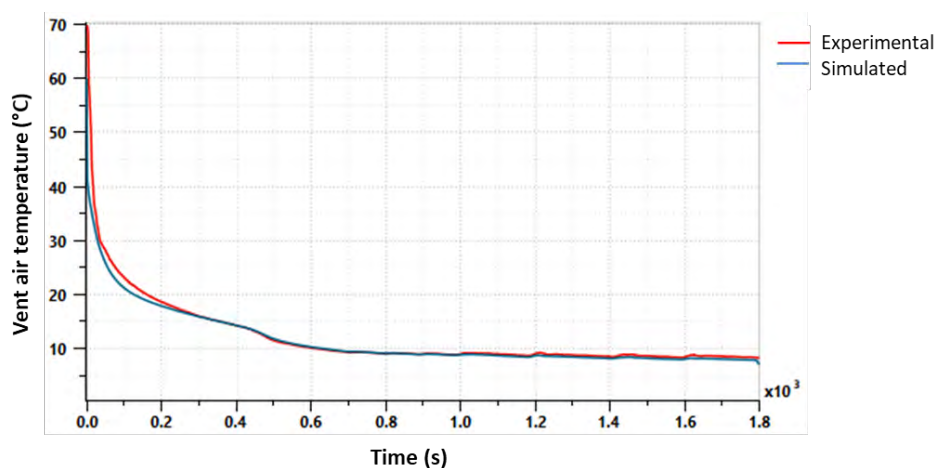


Figure 28: Experimental vs. simulated vent air temperature in cooling mode (climate system calibration model)

Simulated air temperatures at evaporator outlet and vent outlet fit the experimental trends well.

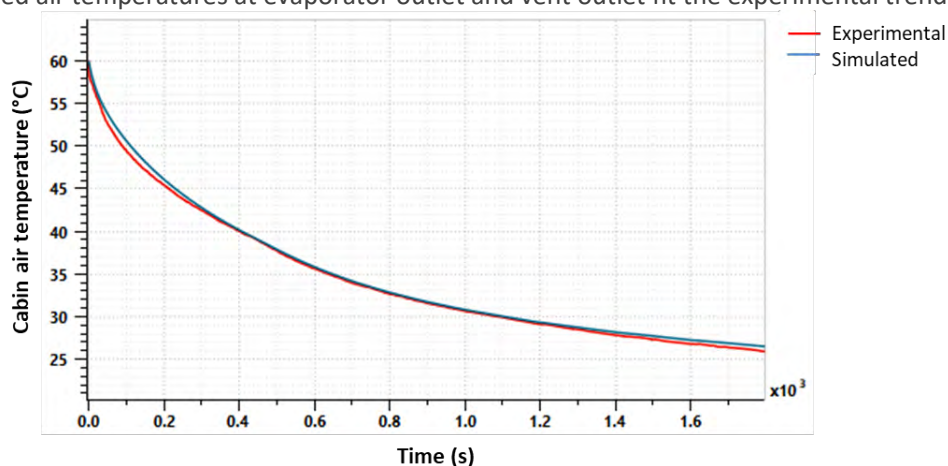


Figure 29: Experimental vs. simulated cabin air temperature in cooling mode (climate system calibration model)

Also the average temperature of cabin air approaches the experimental data with a good accuracy.

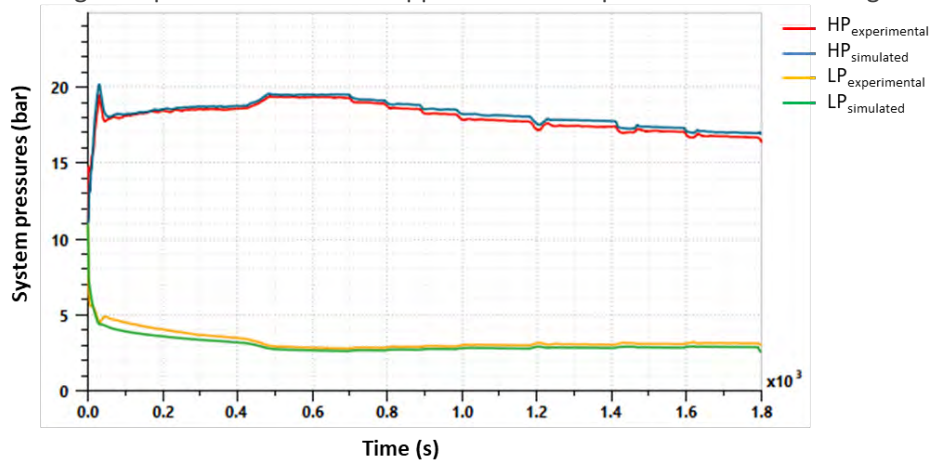


Figure 30: Experimental vs. simulated 2-phase system HP and LP in cooling mode (climate system calibration model)

High and low pressures of two-phase loop approximate the experimental trends well.

### 3.5 1D physical-based model performance

The Real Time (RT) factor is the amount of elapsed time to compute 1 second of simulated time. This is an index of the computational performance of the model.

The RT factors for the simulation models are:

- RT= 0.0076 in WU
- RT=0.25 in CD

The test is performed on a PC with Intel(R) Core(TM) i7-6820HQ CPU @ 2.70GHz processor.

The warm-up simulation is faster than the cool-down simulation for two reasons:

1. During the warm-up test, the HVAC module is in fresh air mode: the air flow enters the HVAC module, then it flows into the cabin, then out of it to the ambient. The air path is an open circuit, without any feedback between the cabin outlet and the HVAC inlet. During the cool-down test the HVAC module is in the recirculation mode: the air path is closed, and then the feedback causes an increase in computation time.
2. The presence of the AC loop into the cool down simulation has a big impact on the simulation time, because the two phase flow equations are highly non-linear (due to the refrigerant properties) and the solver takes a lot of time to solve them, due to reducing the time step size to satisfy the integration accuracy.



The most significant accuracy evaluations, estimated as the difference between the experimental data and the corresponding simulated data, are shown in the following graphs:

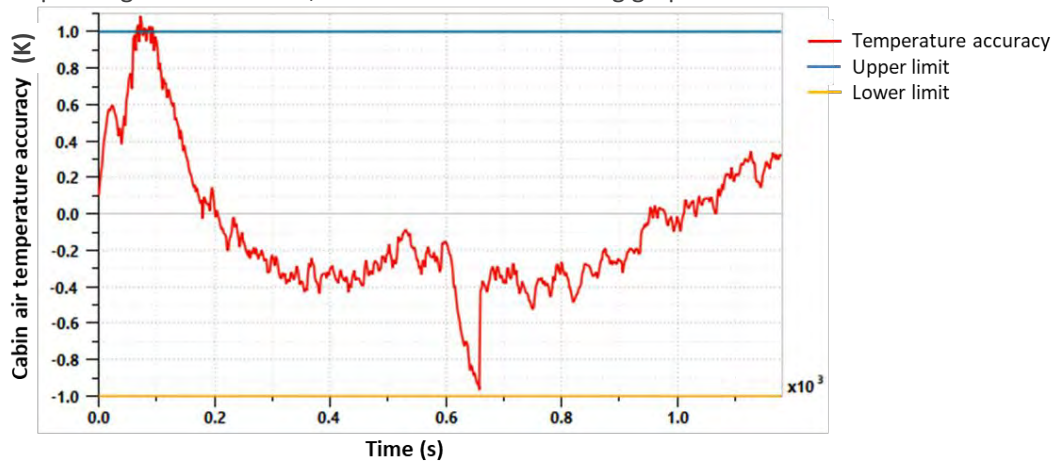


Figure 31: Model accuracy for cabin air temperature evaluation in heating mode

For the heating mode, the climate system model is able to reproduce the average temperature of the cabin air with an accuracy of  $\pm 1$  K ( $RMSE = 0.38$  K or 1.52%).

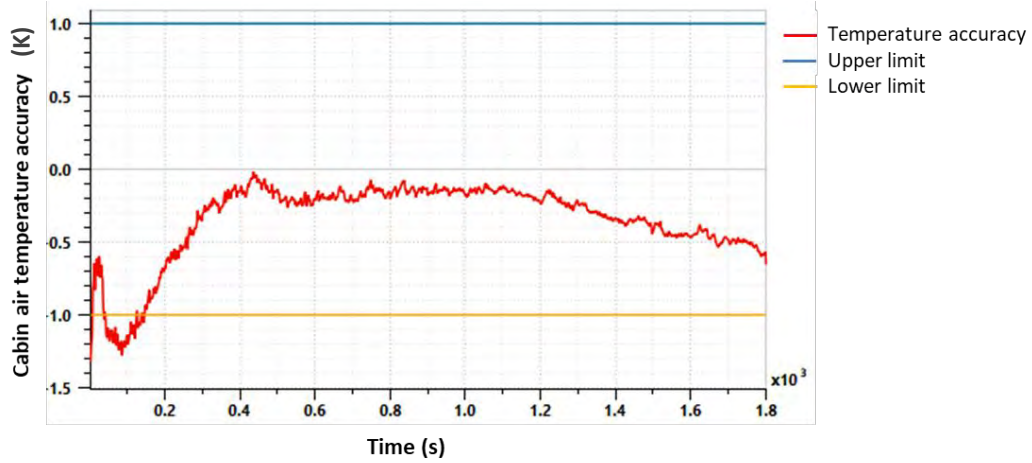


Figure 32: Model accuracy for cabin air temperature evaluation in cooling mode

Also for the cooling mode the climate system model is able to reproduce the average temperature of the cabin air with an accuracy of  $\pm 1$  K ( $RMSE = 0.37$  K or 1.05%).

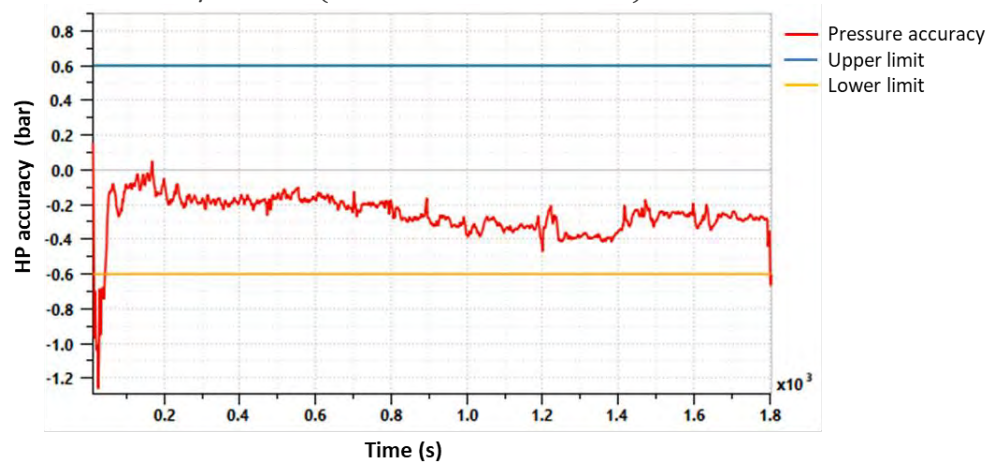


Figure 33: Model accuracy for 2-phase system high pressure evaluation in cooling mode

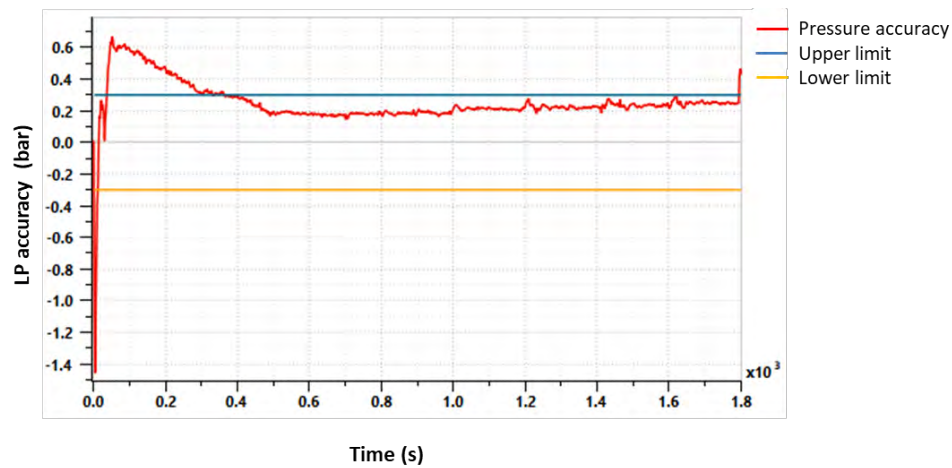


Figure 34: Model accuracy for 2-phase system high pressure evaluation in cooling mode

For the cooling mode, the high pressure accuracy for the considered time interval maintains inside the range  $[-0.6, 0.6]$  bar, corresponding to  $\pm 3\%$ , while the low pressure accuracy varies inside the range  $[-0.3, 0.3]$  bar corresponding to  $\pm 10\%$ , so it is possible to conclude that the model approximates the real behaviour well.

## 4 Efficient model using machine learning (COV)

### 4.1 Introduction

Within Task 1.4, two parallel activities both aim to provide a fast simulation of the thermal dynamics of the car cabin. The first, presented in the previous section, is based on a more traditional, 1D or lumped model. Specifically, the lumped model approach divides the system into a series of components, each of which is modelled using a series of partial or ordinary differential equations. Correct configuration of these equations requires some knowledge of the physical interaction occurring and the thermal characteristics of the materials involved.

The second, presented in this section, aims to provide a comparable simulator that is derived without knowledge of the physical system but rather is entirely obtained from either measurement data or data produced by another simulator. Note that due to delays in the production of a CFD simulation, the first option (measurement data) is used. Specifically, the measurement data used is that produced by CRF using two Climatic Wind Tunnel (CWT) test facilities.

The results show that a high-quality simulator is produced using a simple set of methods that has excellent performance characteristics. The key contribution of this work is to provide a fast, reasonably accurate simulator and to demonstrate the method for use in other parts of the project.

### 4.2 Background

#### Linearity of DEs for thermal systems

When formulated as differential equations, thermal systems are (mainly) linear with respect to their inputs.

Given a simple thermal system that involves a body (such as a container full of water) of temperature  $y(t)$ , an external environment that maintains a uniform temperature  $y_0$  and an insulating barrier (the outer wall of the container) of coefficient  $k$ , the rate of change of temperature of the body  $\frac{dy}{dt}$  is proportional to the difference between the inside and outside temperature, or,

$$\frac{dy}{dt} = -k(y - y_0)$$

This is also known as Newton's model and forms the basis for "lumped" thermal models (models where the components parts (or lumps) are considered to have a single uniform temperature). Note that the coefficient  $k$  might be expanded to consider the surface area and the per unit area thermal resistivity of the wall.

A *transient* simulation, given the current state  $y(t)$ , must identify  $y(t + \Delta t)$  for some small increment in time  $\Delta t$  (say 1 s). An Euler simulation is a numerical approximation that assumes that  $\frac{dy}{dt}$  is roughly equal to  $\frac{\Delta y}{\Delta t}$  and so,

$$\frac{\Delta y}{\Delta t} \approx -k(y - y_0).$$

Given this approximation, for small  $\Delta t$ ,

$$\begin{aligned} y(t + \Delta t) &\approx y(t) + \frac{\Delta y}{\Delta t} \cdot \Delta t \\ &= y(t) - k\Delta t \cdot y(t) + k\Delta t y_0 \\ &= (1 - k\Delta t) \cdot y(t) + k\Delta t y_0 \end{aligned}$$

which is now of the general linear form



$$y(t + \Delta t) \approx m \cdot y(t) + c$$

This allows us to conclude that a simple linear regression between  $y(t)$  and  $y(t + \Delta t)$  would yield the key coefficients in what otherwise appears to be a complex relationship between the internal temperature, the external temperature and the thermal resistivity of the dividing wall.

In summary, the simple thermal problem can be simulated using a linear correspondence between the current state  $y(t)$  and the next state  $y(t + \Delta t)$ .

Finding the coefficients for such a dynamical system is termed *system* or *model identification*.

### Supervised machine learning methods

Although a simple linear correspondence may be sufficient for a simple system, there lies the suspicion that as the complexity of the model increases, non-linearities will appear. Furthermore, some effects, such as radiative heat transfer, are proportional to the fourth power of the difference in temperatures and thus seem to demand a more flexible modelling method.

As suggested by work on non-linear autoregressive systems with exogenous inputs (NARX), some form of neural network or recurrent neural network may be appropriate (Ng, Darus, Jamaluddin, & Kamar, 2014).

Artificial neural networks (ANNs) is the broad term for a set of mathematical modelling constructs that “learn” a mapping from input to output based on a set of supervised examples and which are loosely based on parallels with neurons in the brain. The simplest form is a single layer perceptron that produces a binary output based on some linear function of its inputs and a threshold. Specifically, it corresponds to the function

$$f(\mathbf{x}) = [\mathbf{w} \cdot \mathbf{x} + b > 0]$$

where  $[\cdot]$  is the indicator function and returns 1 if the condition is true and 0 otherwise.

Depending on the application, the threshold mechanism or *activation function* can be varied. Commonly used activation functions include *ReLU* (rectified linear unit), *sigmoid*, *tanh*, and pass through or *linear*.

ReLU is a relatively modern activation function that has had success as a hidden layer activation for problems such as handwriting recognition. Sigmoid and tanh are commonly used smooth, differentiable functions whereas linear activation merely passes through the input without modification.

Table 1 Summary of neural network activation functions

Activation	Formula
linear	$f(x) = x$
ReLU	$f(x) = \max(0, x)$
sigmoid	$f(x) = 1/(1 + \exp(-x))$
tanh	$f(x) = \tanh(x)$

ANNs are often displayed diagrammatically as arcs and nodes, as shown in the following diagram.

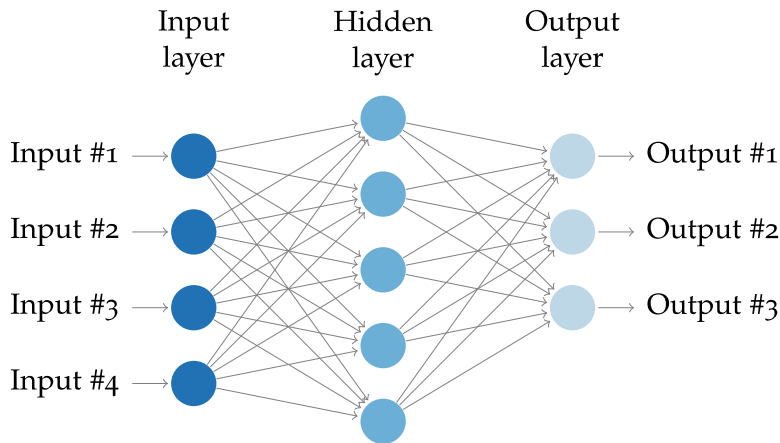


Figure 35 Example ANN involving 4 inputs, 1 hidden layer with 5 nodes in the hidden layer, and 3 outputs

Each arc in the network has an associated weight  $w_{i,j}$ . For example, for 7 inputs and 4 outputs, the weights can be expressed as a matrix  $W$  with dimensions  $7 \times 4$ . For linear activation (or pass through) on the output nodes, the general form is,

$$\mathbf{y} = \mathbf{W}\mathbf{x} + \mathbf{b}$$

Naturally, other activation functions and the addition of hidden layers with varying numbers of nodes per layer produce a non-linear function of arbitrary complexity and expressiveness.

A key insight in this work is to realise that many physical systems can be predicted using only the current state and control inputs. In some cases, the prior state is also needed (e.g., as a proxy for the velocity of a moving object where the state contains just its position). Therefore, the structure of the simulator is a transfer function of the form,

$$\mathbf{x}_{t+1} = f(\mathbf{x}_t, \mathbf{u}_t)$$

which is mapped to the neural network by presenting the combined state and control  $(x_{t,1}, x_{t,2}, \dots, u_{t,1}, u_{t,2}, \dots)$  as the input, and  $\mathbf{x}_{t+1}$  as the output. Learning  $f(\cdot)$  then provides a simulator.

The next section describes the preparation of the input data, while the following section gives the performance results for the resulting simulator.

### 4.3 Method and materials

- Five CWT trials were performed in 2 different test facilities.
- Although CAN data was collected during some of the trials, for consistency this data was ignored. Furthermore, some other measurement values were not consistently collected during all trials and were thus ignored for those trials where they were collected. This includes thermocouple sensors 138, and 154, (both underfloor sensors) and also the wind velocity.
- Due to the different test facilities, some data was collected at 1 Hz (tests 2 and 5), while other data was collected at 0.1 Hz. The higher sample rate data was therefore resampled at 0.1 Hz.
- Some noise is apparent in most signals and to ease the machine learning task this is reduced by using a rolling mean with window of 50 seconds.
- Further specification of the settings used during the test is as follows:

#### CWT1

1. Fresh air
2. HVAC Auto at T cabin 22°C
3. Defroster + Floor
4. 60 min at 50 km/h; 120 min vehicle off

## CWT2

1. Recirculation, afterward Fresh air
2. HVAC Auto at T cabin 22°C
3. Vent in neutral position
4. 30 min in Rec. air at 100 km/h; 30 min in Fresh air at 100 km/h; 120 min vehicle off

## CWT3

1. Air distribution in auto.
2. HVAC Auto at T cabin 22°C
3. Defroster + Floor
4. production of 140 g/h of moisture into the cabin
5. 30 min in Rec. air at 100 km/h; 30 min in Fresh air at 100 km/h; 30 min vehicle off

## CWT4

1. Fresh air
2. HVAC Auto at T cabin Max Cold
3. Defroster + Floor
4. 60 min at 50 km/h; 120 min vehicle off

## CWT5

1. Recirculation, afterward Fresh air
2. HVAC Auto at T cabin Max Hot
3. Vent in neutral position
4. 30 min in Rec. air at 100 km/h; 30 min in Fresh air at 100 km/h; 120 min vehicle off

The above settings were resolved into three additional variables (one for whether fresh or recirculation mode, another for neutral versus defrost / floor air distribution, and a third for velocity).

## Control vector

From the measurement datasets, the following columns are taken as control inputs:

- vent input air temperatures: sensors 49–58 and 81–82
- the blower amperage
- the external roof temperature: sensor 26<sup>1</sup>
- the ambient air temperature
- the ambient relative humidity
- the car velocity
- the fresh/recirc and distribution setting (neutral or defrost / floor).

A total of 19 control inputs, as listed above, are used. These inputs include elements that are directly controlled by the HVAC controller (such as the blower amperage and distribution setting), elements that are indirectly controlled and whose control needs to be separately modelled (the vent input air temperatures), and elements that are not controlled, affect the cabin temperature, and can be measured, such as the car velocity.

## State vector

The state of the system is represented by a vector containing:

- sensors 161–172 for the air and mean radiant thermocouples attached to front driver and passenger head, torso, and foot. Specifically,

---

<sup>1</sup> This sensor was included to substitute for the lack of a solar sensor. For example, ambient air temperature might be cold, but the car still heats up due to incident solar radiation. In principle, a suitable solar sensor input might be substituted here.

- 161: driver head air temperature
- 162: driver head mean radiant temperature
- 163: driver torso air temperature
- 164: driver torso mean radiant temperature
- 165: driver foot air temperature
- 166: driver foot mean radiant temperature
- 167: passenger head air temperature
- ...
- 172: passenger foot mean radiant temperature
- windshield (driver side) temperature sensor (39)
- relative humidity inside the cabin
- anemometer readings for driver / passenger at the head, torso and foot locations.

The state vector contains 20 elements.

### Additional input information

To further improve performance, the previous state is also provided as input. For example, given successive states  $\mathbf{x}_1, \mathbf{x}_2, \dots$ , the neural network is posed the problem as a function of the two immediately prior states  $\mathbf{x}_t, \mathbf{x}_{t-1}$ , the control input  $\mathbf{u}_t$ , to map to the current state  $\mathbf{x}_{t+1}$ , or, in other words, to find parameters  $\boldsymbol{\theta}$ , where

$$\mathbf{f}(\mathbf{x}_{t-1}, \mathbf{x}_t, \mathbf{u}_t, \boldsymbol{\theta}) \approx \mathbf{x}_{t+1}$$

The rationale for providing this additional input is that there may be some inertia in some of the state variables involved. For example, an air velocity that has been increasing will tend to increase for a short while even if the control inputs are changed.

### Identifying the best model

Having assembled the data, the next step in the method is to identify the best learning structure. The method used is a random hyper-parameter search. An alternative might be to use an evolutionary algorithm to find the optimal hyper parameters.

A hyper parameter search aims to identify the best model structure for the neural network with a Multi Layer Perceptron or Deep Neural Network architecture. The elements that can be altered are:

- number of hidden layers (0 to 4)
- activation for hidden layers (ReLU, sigmoid, tanh, linear)
- activation for final layer (same)
- number of nodes in each hidden layer (1-500)
- whether a dropout regularisation is used (0.5 if yes)

Note that the limits placed on the search (values in brackets) are somewhat arbitrary but necessary to constrain the search space.

The network is learnt using TensorFlow (“TensorFlow,” n.d.) and Keras (“Home - Keras Documentation,” n.d.) with the Adam optimizer aiming at minimising the mean square error. From the hyper-parameter space given above, 200 variants are selected at random (with uniform distribution for number of nodes), with 10-fold cross validation. Input and outputs are rescaled to a unit range using min-max rescaling. The data is preprocessed as discussed previously (see start of section 4.3) to smooth, sparsify, and ensure a constant periodicity.

Note: for this work, the data-set was quite limited and it was not possible to hold-back an unseen test set for further validation of the model selection, as suggested by Nowotny (Nowotny, 2014) (i.e., 2 layer cross-fold validation). For this work, k-fold cross-validation was used to establish the best model structure and then the full dataset was used to both produce and test the resulting model.

## 4.4 Results

### Model search results

The top performer is a simple linear, zero hidden layer network with mean MSE of  $0.00024 \pm 0.00002$  for 10 second prediction of min-max rescaled data. Due to the rescaling required for the neural network, the MSE is already normalised. Thus, it translates to a normalised RMSE (or NRMSE) of  $\sqrt{0.00024} \cdot \frac{100}{1} \% = 1.5\%$  over 10 seconds. Note that the prediction error for several hours of simulation is likely to be larger.

The simple zero-hidden-layer (or perceptron) network roughly corresponds to a linear predictor. Therefore a natural alternative to try is linear regression (LR). LR often outperforms the corresponding neural network as it avoids some of the complication associated with stochastic gradient descent that is required for backpropagation in a general NN.

As with the perceptron, LR uses a minimal set of coefficients to model the system. This means that overfitting is unlikely although there may be some possibility of underfitting (not providing sufficient flexibility in the model). Another side effect of this is that the model is robust to measurement noise. Note however, that when sensor readings used as input to LR contain large amounts of noise, the LR estimate of the gradient will be smaller than the true value. Thus, it is still useful to minimise noise to get the best model.

In the following section, we explore the hyper-parameter results in more detail before coming back to the results for LR.

#### 4.4.1.1 Overview of results

The following graph provides an overview of the results from the hyper parameter search. The main results shown here are that, for those network structures that perform poorly, such as those with ReLU as the final activation layer, dropout helps considerably. Dropout is a regularisation technique that disables connections in the network with a fixed probability. This approach is often helpful in dealing with large, highly correlated inputs by making the network less reliant on individual inputs and thus more robust.

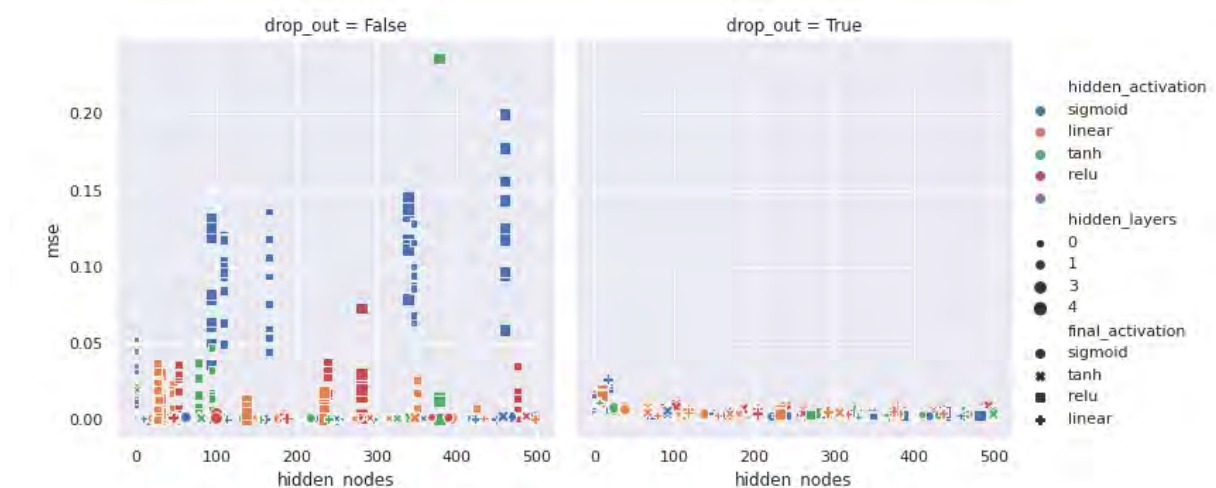


Figure 36 Overview of hyper parameter search

A summary of final activation results shows that ReLU is the worst performer but there is not much difference between the other three. Dropout helps ReLU but makes the others worse.

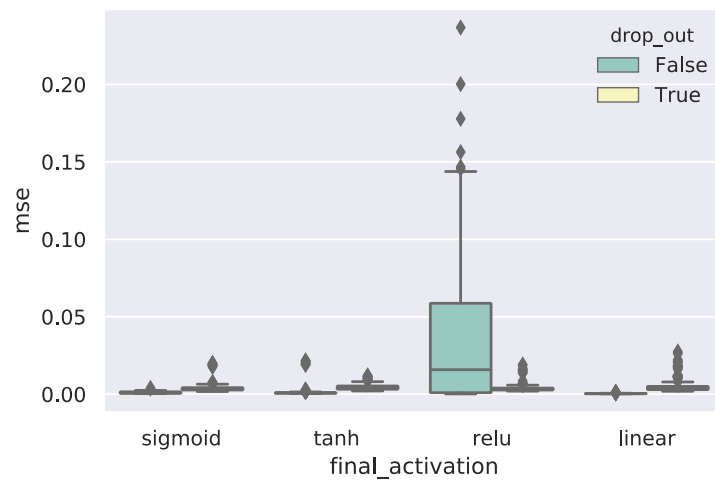


Figure 37 ReLU performs poorly but is helped by dropout whereas other activation functions work better without dropout

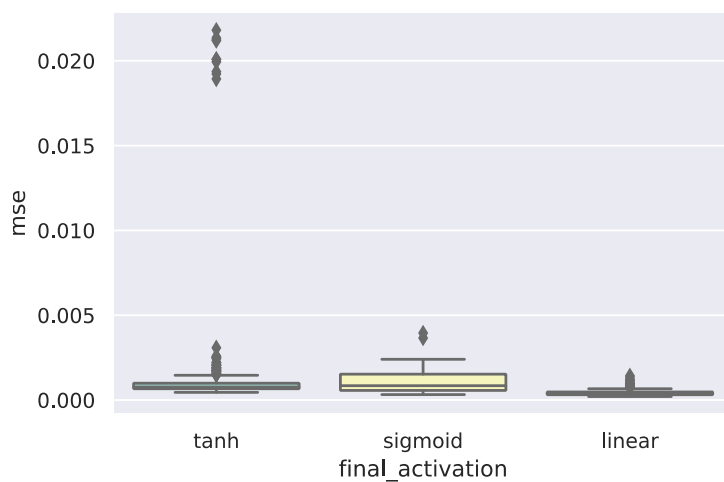


Figure 38 Taking away ReLU and dropout results shows that linear activation is the best performer of the remaining 3 options for final activation

Given linear final activation, no dropout and at least one hidden layer, the choice of hidden activation is between linear and tanh.

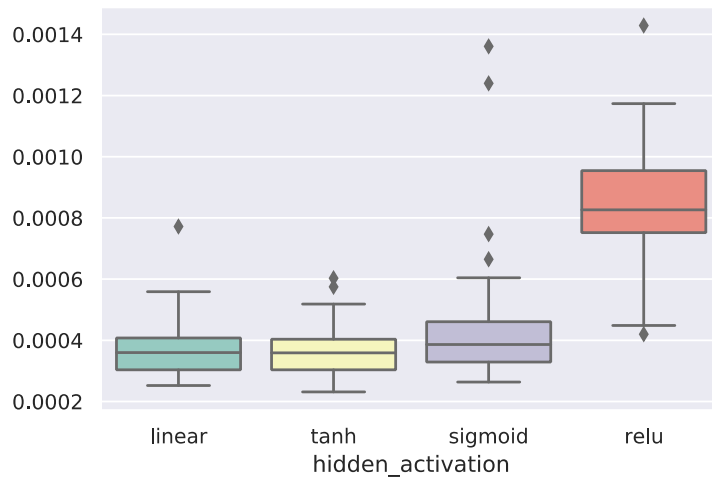


Figure 39 No significant difference (based on the boxplot) between linear and tanh hidden activation for linear final activation without dropout. Sigmoid is slightly worse whereas ReLU is much worse.

The top 10 performers of the hyper parameter search are shown in the table below. The MSE is given as mean  $\pm$  standard deviation over the 10-fold cross-validation. The best performer is a simple perceptron system (single layer of linear activation). This is equivalent to a linear function between inputs and outputs, which thus suggests that linear regression (LR) may also be effective.

Table 2 Top 10 results from hyper parameter search showing that best performer is a linear network with no hidden layers

Hidden nodes	Hidden activation	Final activation	Drop out	Hidden layers	MSE
0	NA	linear	FALSE	0	0.00024 $\pm$ 2e-05
155	tanh	linear	FALSE	2	0.00029 $\pm$ 4e-05
346	linear	linear	FALSE	1	0.00030 $\pm$ 3e-05
277	tanh	linear	FALSE	1	0.00030 $\pm$ 5e-05
161	sigmoid	linear	FALSE	2	0.00033 $\pm$ 4e-05
113	sigmoid	linear	FALSE	2	0.00033 $\pm$ 4e-05
240	tanh	linear	FALSE	2	0.00036 $\pm$ 6e-05
163	tanh	linear	FALSE	3	0.00036 $\pm$ 5e-05
296	tanh	linear	FALSE	2	0.00038 $\pm$ 7e-05
52	tanh	linear	FALSE	4	0.00038 $\pm$ 5e-05

Linear regression does not require rescaled data but, for the purposes of comparison, 10-fold cross validation LR on rescaled data gave an MSE of  $0.00015 \pm 1e-05$  thus significantly outperforming the best performing neural network. LR is thus chosen as the best fitting model for this data.

### Evaluation of the best performing model

The LR model trained with unscaled data can then be examined in terms of:

- How well simulation produced for longer periods compare with CWT data
- Normalised root mean square (NRMSE) results for whole trials
- Compute performance

#### 4.4.1.2 Simulation results comparing simulator with original data

The following figure shows a comparison of simulation output with measurement data for sensor 161 (head air temperature for the driver) during CWT trial 1. The correspondence is remarkable since there is no divergence between two curves—there is only a small error between them—even over the extended period of the test (around 3 hours). Furthermore, the temperatures vary over a large range during the trial from almost 0 deg C at the beginning to a peak of nearly 30 deg C.

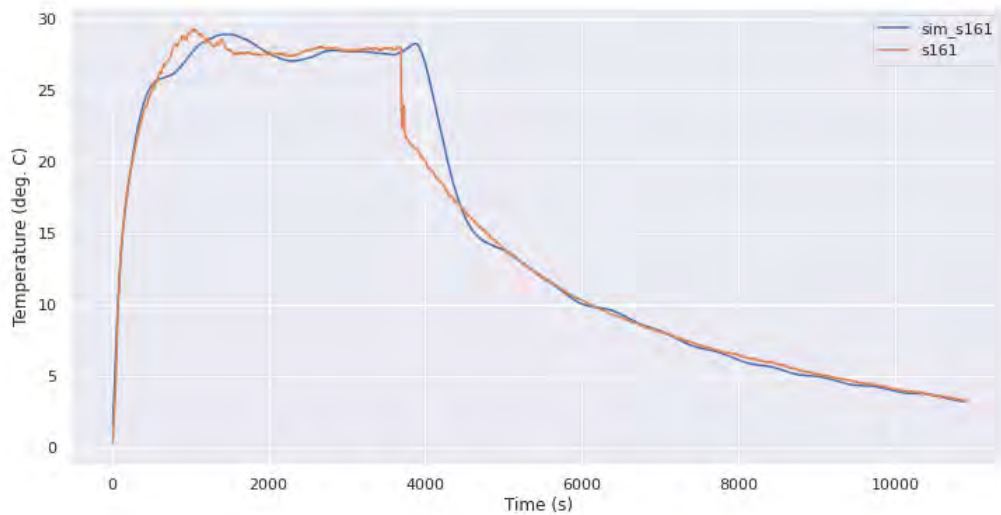


Figure 40. Comparison of simulation produced curve for sensor 161 versus measurement data from CWT (without smoothing).

Other sensor modalities appear to be reproduced with similar accuracy. The following graph shows relative humidity within the car cabin. Again, this is striking as the relative humidity varies over a wide range during the trial. The simulator manages to track it almost perfectly just on the basis of the initial state and the control inputs.

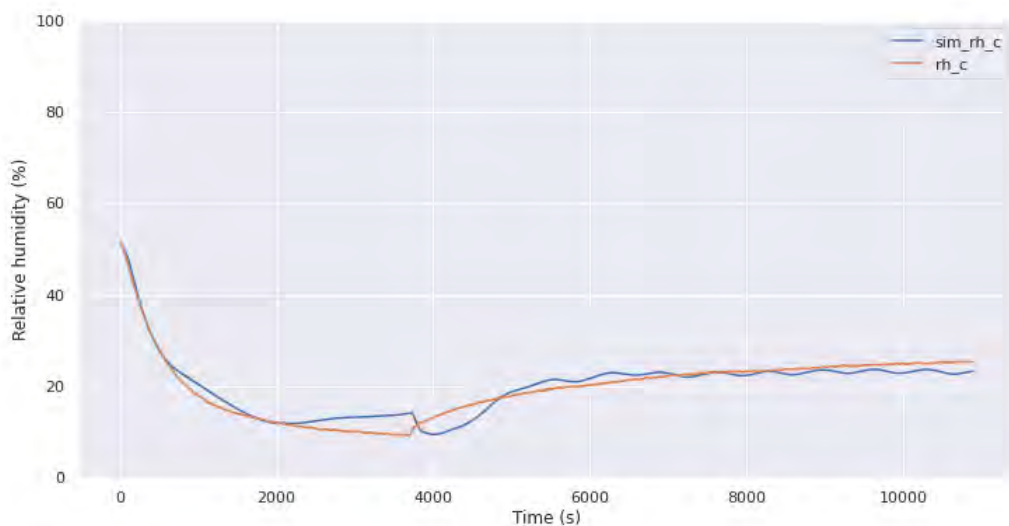


Figure 41. Simulation versus CWT for relative humidity



Air velocity measurements tend to vary considerably. These measurements are smoothed during processing and thus the simulator produces a smooth estimate of the air velocity. The following graph corresponds to the anemometer at the driver's head. The correspondence here is quite consistent through the whole period.

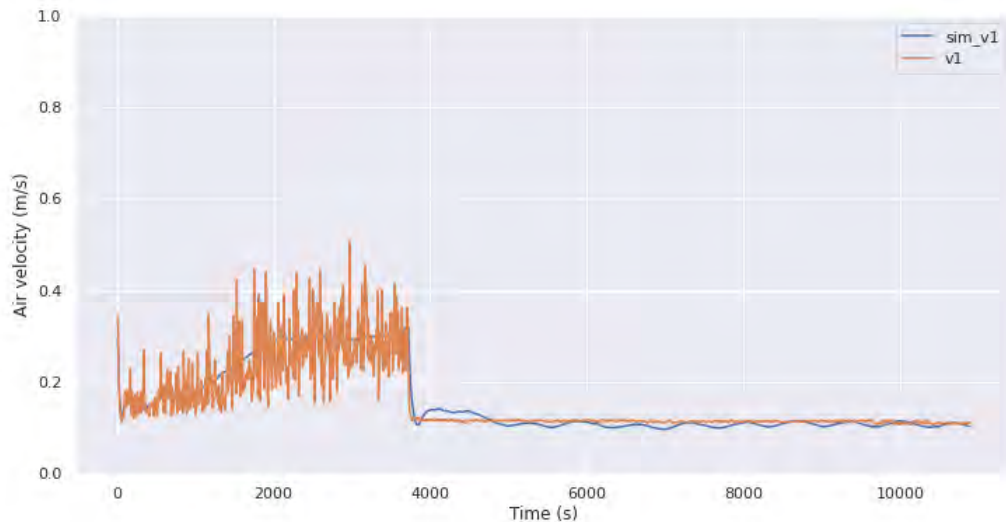


Figure 42. Simulation versus CWT for air velocity at driver's head

#### 4.4.1.3 Differences between head, chest, and foot temperatures

A key benefit of the ML-simulation approach is the ability to differently estimate different parts of the cabin space. For example, the temperature at the head may be much hotter than the footwell and this difference affects thermal comfort. Therefore, it is interesting to see whether the simulation is able to independently and differently track the air temperature (for example) at the head, torso and foot. The following graph demonstrates that this tracking is very good. In particular, notice that the footwell (s165 and sim\_s165) is higher than the head and torso locations during the first part of the trial while the long term progression (where the HVAC was turned off after 4000 seconds) ended with clearly separate temperatures for the three locations and that all were correctly predicted by the simulator.

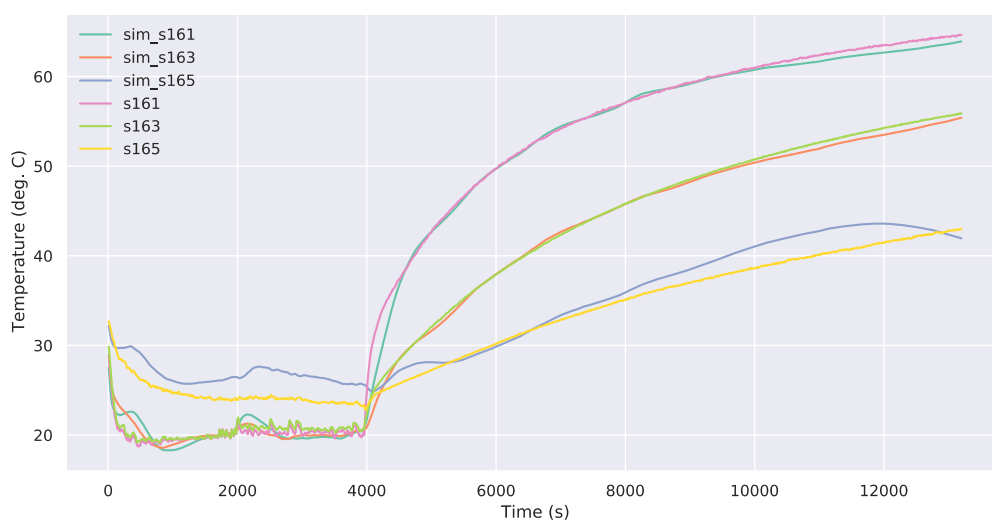


Figure 43. ML-simulator correctly and independently tracks driver's head (s161), chest (s163), and foot (s165) temperatures over a 3 hour trial (CWT2) with only small errors.

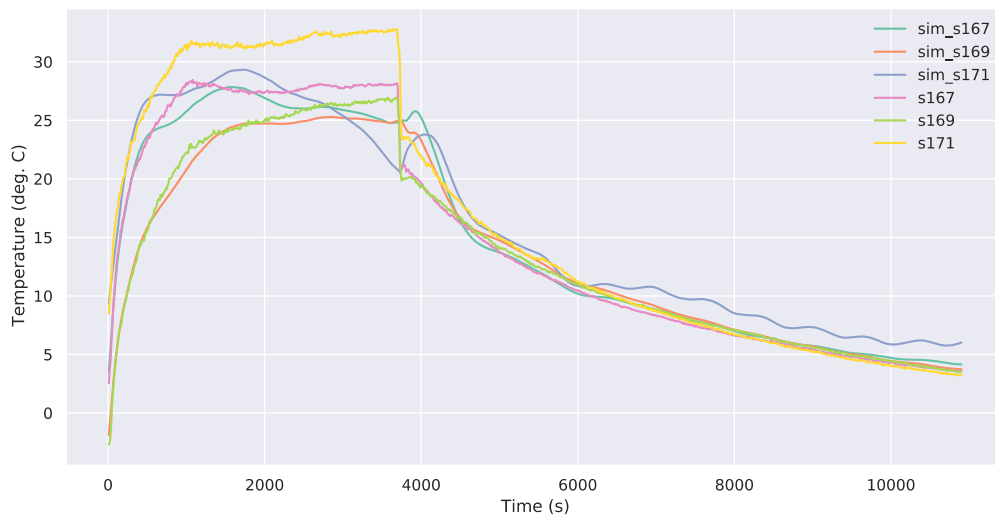


Figure 44. Passenger side air temperatures are reasonably accurately tracked with clear differences during the early phase between head (s167), torso (s169), and foot (s171) for trial CWT1.

#### 4.4.1.4 Examples showing room for improvement

The following example shows some response differences in the simulator compared to the CWT data. Note that the vertical range is small and this may appear to magnify errors. A striking aspect of this result is that the final temperature converged upon is very close to the true final temperature.

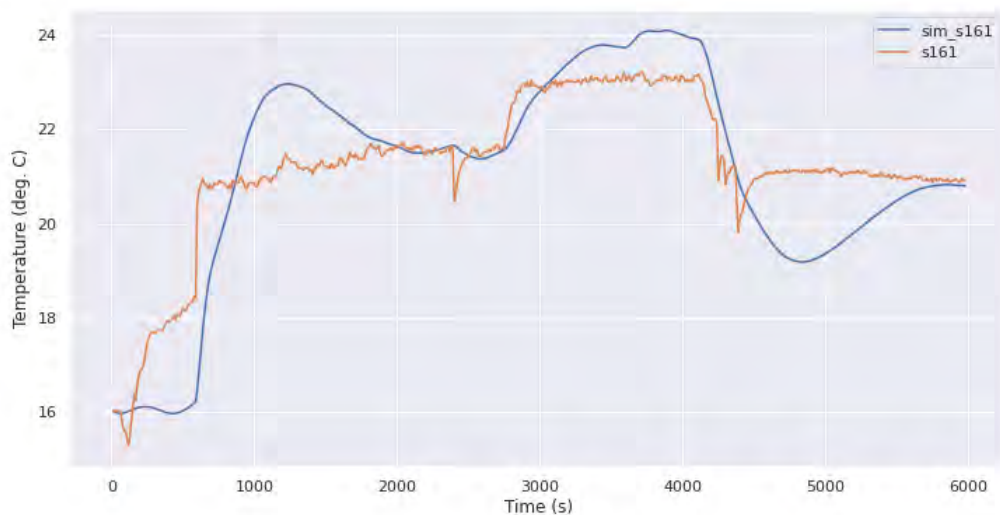


Figure 45. Comparison for CWT trial 3 Sensor 161 (driver head air temperature)

Another example is the windshield temperature simulation for CWT trial 3. Here the temperatures are quite stable during the CWT trial but vary considerably in the simulation. Again, the vertical range is small but the error is up to 3 degrees C.

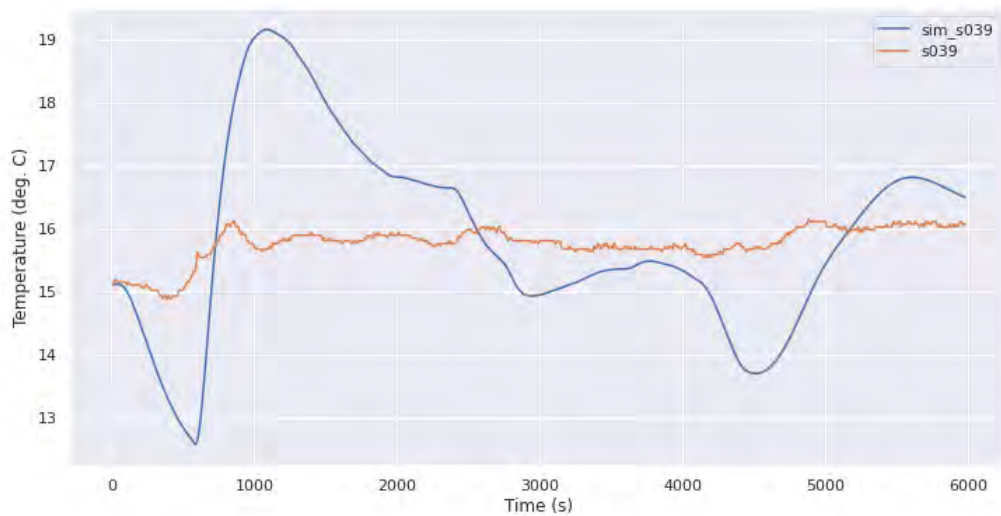


Figure 46. Comparison for CWT trial 3 Sensor 39 (windshield temperature driver's side)

It might reasonably be expected that better performance of the predictor would be obtained by providing more data.

#### 4.4.1.5 NRMSE results

Rather than trying to understand the accuracy of the simulation based on examining individual graphs, it is generally more appropriate to summarise the error in terms of the RMSE or NRMSE (as described in appendix 1). The following table of results were obtained by running the simulator for each of the CWT trials. The RMSE and NRMSE shown here is the mean  $\pm$  the standard deviation over the 5 trials. Note that NRMSE is shown as a proportion rather than a percentage. For example, an NRMSE of 0.004 corresponds to 0.4%. The RMSE and NRMSE values here are for the full trials (around 3 hours each) and thus will be somewhat larger than the 10 second prediction RMSE or corresponding MSE used during training. The units for the RMSE depend on the sensor: The thermocouple RMSE values (sensors starting "s...") are in kelvin; rh\_c is in percentage relative humidity; air velocity (sensors starting "v...") is in m/s. The table is ordered according to mean NRMSE. Note that the displayed decimal places are adjusted according to the standard deviation.

The average NRMSE performance over all sensors over the full trial duration is 0.018 (or 1.8%), which is comparable but slightly larger than the 10 second NRMSE (1.5%). The average air temperature RMSE is 0.4 K or 0.8%.

*Table 3. Performance of machine-learnt simulator in terms of error for each sensor. Average air temperature (avg\_air) is based on comparing the average of head, torso and foot air temperatures for driver and front passenger with that of the simulated values. The table is sorted by NRMSE.*

Sensor	RMSE	NRMSE
s170	0.29 ± 0.1	0.004 ± 0.001
s162	0.35 ± 0.09	0.005 ± 0.001
s169	0.3 ± 0.1	0.005 ± 0.002
s168	0.4 ± 0.1	0.005 ± 0.002
s164	0.35 ± 0.08	0.005 ± 0.001
s163	0.31 ± 0.1	0.005 ± 0.002
s161	0.4 ± 0.1	0.007 ± 0.002
s167	0.5 ± 0.2	0.007 ± 0.003
avg_air	0.4 ± 0.2	0.008 ± 0.003
s039	0.6 ± 0.3	0.009 ± 0.004
s172	0.8 ± 0.4	0.016 ± 0.007
s166	0.8 ± 0.4	0.016 ± 0.008
rh_c	0.7 ± 0.2	0.017 ± 0.005
s165	0.8 ± 0.4	0.019 ± 0.009
s171	1.1 ± 0.5	0.02 ± 0.01
v1	0.04 ± 0.03	0.03 ± 0.03
v6	0.040 ± 0.009	0.029 ± 0.007
v2	0.03 ± 0.01	0.04 ± 0.02
v4	0.04 ± 0.01	0.04 ± 0.02
v3	0.032 ± 0.007	0.043 ± 0.01
v5	0.03 ± 0.01	0.04 ± 0.02

#### 4.4.1.6 Holistic comfort model performance

The aim is for the simulator to be able to estimate holistic comfort within 10%. We show results obtained here for the driver but similar results are obtained for the front passenger. The full description of the DOMUS Holistic Comfort Model (HCM) is given in deliverable 1.3. This model results in two forms: one is a full model that includes all possible elements and the other is a reduced model that is restricted to measurable sensor values. The reduced model is used here.

The reduced model requires the following inputs:

- body\_state - 3 x 3 array containing head, torso, foot: air temperature, mean radiant temperature, air velocity
- pre\_out - outside temperature (degree Celsius)
- pre\_clo - clothing insulation (clo)
- qa\_ht - height of cabin occupant (cm)
- qa\_wt - weight of cabin occupant (kg)
- rh - relative humidity (m/s)
- co2ppm - carbon dioxide concentration (ppm)
- sound - sound level (dBi)

- light\_blue - binary variable indicating whether ambient light is blue (1 for Blue, 0 otherwise)
- light\_yellow - binary variable indicating whether ambient light is yellow (1 for Yellow, 0 otherwise)
- scent\_OC - binary variable indicating whether scent is Orange and Cinammon (1 for OC, 0 otherwise)
- scent\_Pepper - binary variable indicating whether scent is Peppermint (1 for Peppermint, 0 otherwise)

Given the absence of information about the occupant in this case, and no scent, colour, sound-level, or CO2 information, nominal values are assumed for those. Specifically, clothing level (pre\_clo) is assumed to be 0.7, height 178, weight 89, lux 5, co2ppm 450, sound 0, colours and scents are zero.

For the last 2 trials, the HCM always predicts that the driver is uncomfortable (for both simulated and real measurements) and so these two trials are not included in the results below.

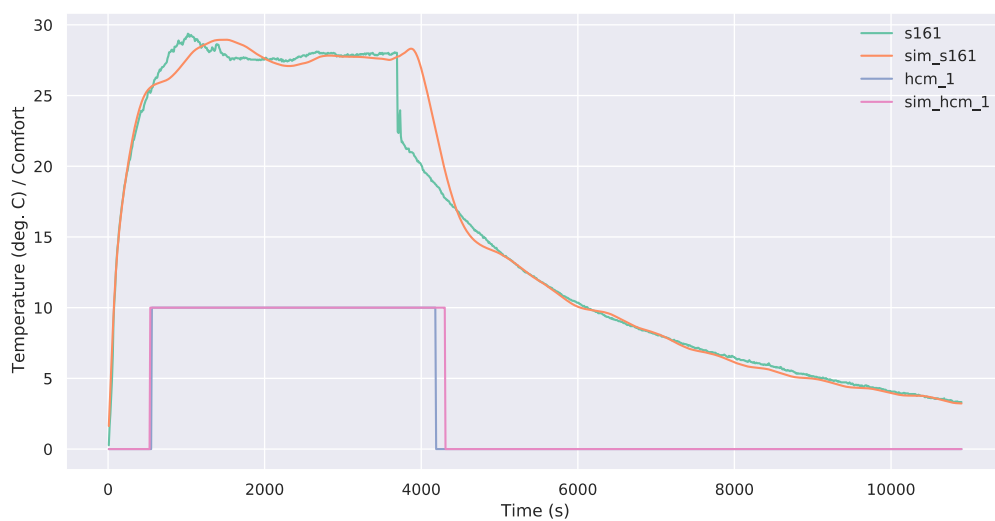


Figure 47. CWT-1 simulated versus measurement for driver head temperature and HCM comfort score. The HCM score is converted to an integer and multiplied by 10 to show on the same axis. Note that the simulated estimate lags the true value of the cabin temperatures and this is reflected by a lag in the simulated HCM score.

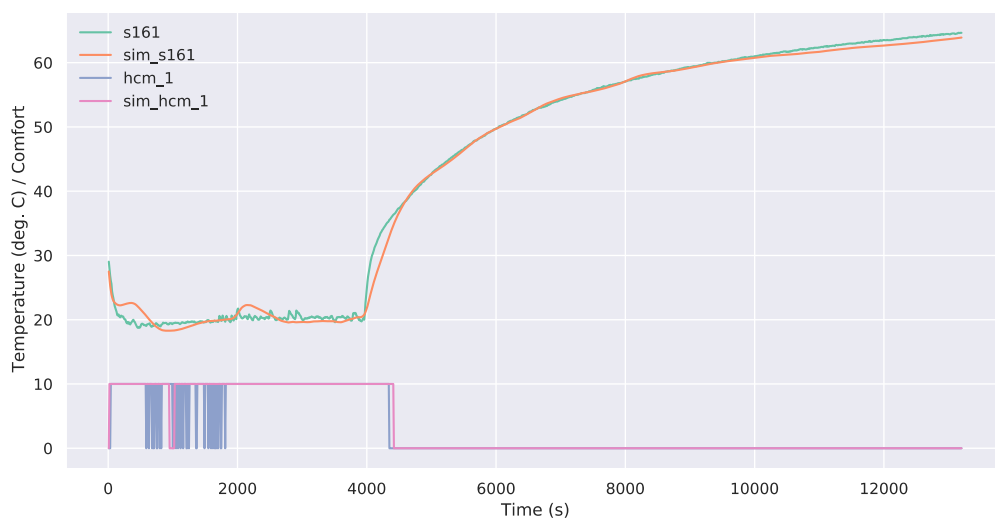


Figure 48. CWT-2 simulated versus measurement for driver head temperature and HCM comfort score. Around the 1000 s mark, the temperatures come close to the HCM's threshold causing the HCM to oscillate rapidly between comfortable and

uncomfortable. This is partly due to noise in the sensor measurement. The simulated values are smoothed and thus do not see such oscillation.

The overall results for the HCM comparison are provided here as a set of confusion matrices, one per trial, that show the incidence of misclassification (both false positives and false negatives).

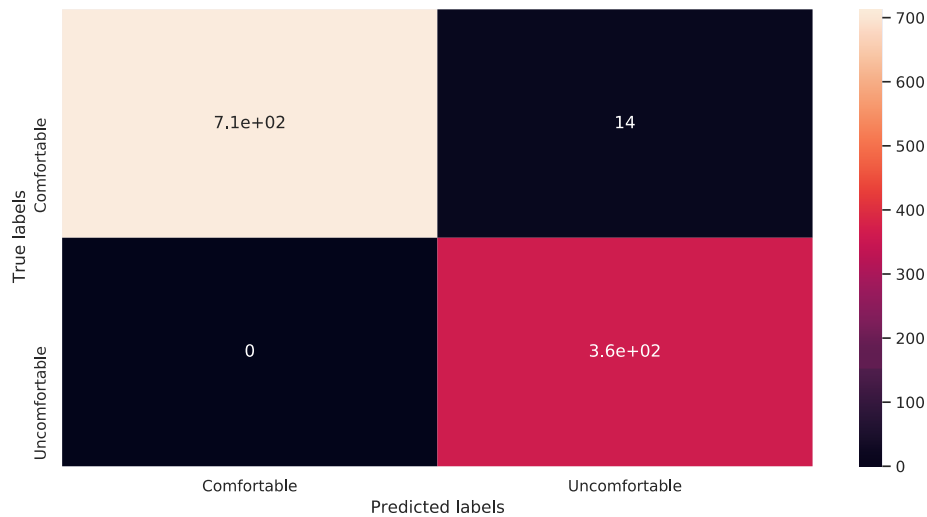


Figure 49. CWT-1 HCM confusion matrix between the HCM based on measurement (or "true" labels) versus the HCM based on simulated measurement (termed "predicted"). Only 1.3% total are misclassified.

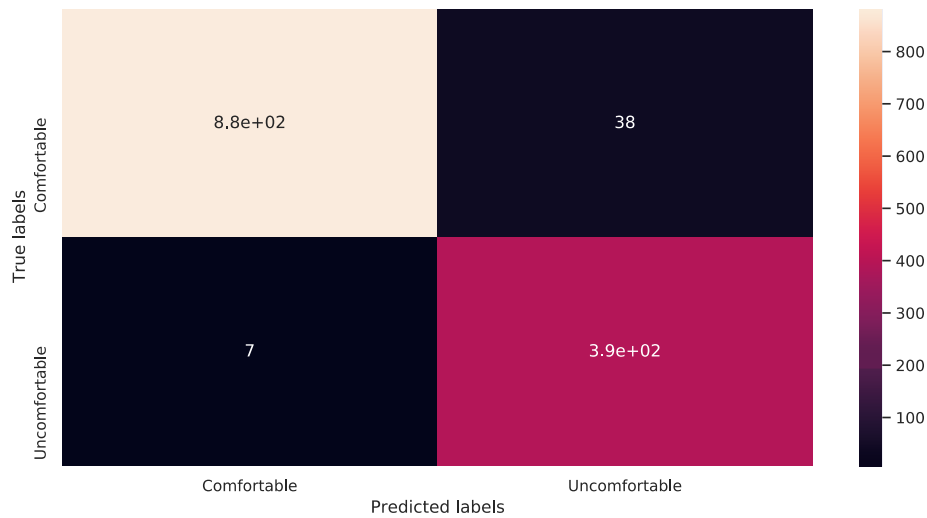


Figure 50. CWT-2 HCM confusion matrix. In this case, 3.4% are misclassified.

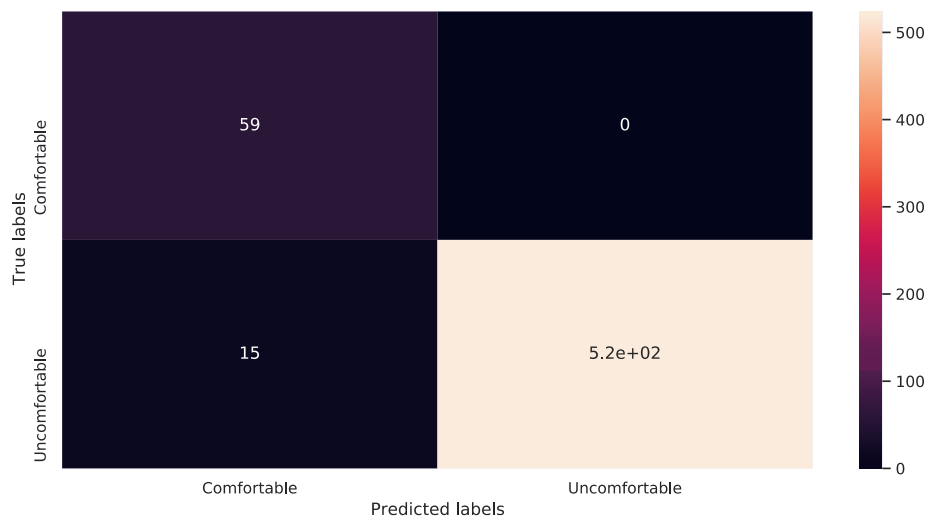


Figure 51. CWT-3 HCM confusion matrix. In this case, 2.5% are misclassified.

In summary, the misclassification rate for the HCM due to simulation error is well below the target of 10%.

#### 4.4.1.7 Compute performance

Calculating a single time step (10 seconds) with the simulator developed in this work is extremely fast. The reason for this good performance is that the calculation can be performed with a single matrix multiplication. Also, LR, unlike the neural network, does not require rescaling of inputs and outputs. On a PC with Intel(R) Core(TM) i7-4790 CPU @ 3.60GHz processor, 1000 × 3 hour simulations were calculated in 59.3 seconds. This corresponds to 5.44  $\mu$ s elapsed time per simulation second (RT 5.44 × 10<sup>-6</sup>).

Compute performance becomes critical when attempting to use machine learning to optimise a control algorithm. In past work, around 9 years of simulated time was required to find the optimal control strategy. The time to compute 9 years of simulated time using this simulator is around 25 minutes.

#### 4.4.1.8 Discussion

These results show a surprisingly high accuracy for this simulator over all the sensors. The smallest errors are less than the expected error in the thermocouple sensor while the largest errors (around 0.04 m/s or 4% of the range) are within the target for the deliverable (within 5% of the accuracy of the high-level model). Thus, this method of producing a simulator easily exceeds the target for accuracy.

The results also reflect that short-term errors tend to disappear over time. This is surprising because, in many simulations, small errors accumulate when producing a simulation that runs over an extended period. This reflects the relative simplicity of the model causing it to be extremely robust.

Possible threats to validity of the LR simulation results are as follows:

- These results are specific to the range of parameters varied during the CWT trials. For example, only 2 distribution modes were switched between—it would not be possible to use this simulator to simulate other distribution modes.
- Similarly, within the DOMUS project, it is expected to add radiant panels and other options that will impact the thermal dynamics. These trials do not include such features and thus could not be used to simulate them. The aim, however, is to apply this method to CFD-based data, which would allow the inclusion of these extra features. Unfortunately, the CFD data was not ready in time to include it in this deliverable.
- A better estimate of the performance on unseen data might be possible using k-fold cross-validation. Since the full data-set was used to both learn the linear regression coefficients and to assess

performance, the true performance on unseen data may be slightly worse than estimated here. Note, however, that overfitting is unlikely for this method. For the final CFD-based simulation, k-fold cross-validation will be used for final evaluation of the simulation model.

## 4.5 Summary

- The best performing machine-learnt simulator is based on linear regression and gives an average, whole trial normalised RMSE of 1.8%.
- The simulator closely tracks thermal, relative humidity, and air velocity dynamics within the cabin and clearly demonstrates the viability of the method.
- For the purposes of WP 2 and 5, this simulator provides a solid basis for work where it is not necessary to add components such as radiant panels.
- Furthermore, this work is remarkable in that it provides a simulator that is capable of accurately simulating the thermal dynamics at multiple car seating positions and to do so with a compute performance that is much faster than traditional 1D approaches. This opens the way for numerical optimisation approaches to building car cabin HVAC controllers (WP5.1.2) and to redesigning the car cabin features (WP2.3) that were previously considered infeasible.
- Future work is required to provide data that can enable simulation of optional components including radiant panels, heated seats, and special glazing. This work is currently on-going as part of Task 1.3.



## 5 Performance of the two models (COV/CRF)

### 5.1 Comparative performance in terms of accuracy

The average NRMSE over all sensors being estimated for the ML-simulator is 1.8%. The best estimated sensor has an NRMSE of 0.4% while the worst has a 4.0% NRMSE. The accuracy of the estimate of the average temperature over the front bench of the car cabin is 0.4 K (0.8%).

The 1D model NRMSE is 1.5% for the temperature. In case of AC loop on, the model performs about 3% for the high pressure and 6% for the low pressure.

### 5.2 Comparative performance in terms of computational speed

The compute performance is measured in terms of the time taken to compute 1 simulation second and this value is termed the RT factor.

The RT factors for 1D simulation are:

- $RT = 0.0076$  in WU
- $RT = 0.25$  in CD

The difference between the two reflects the complexity of simulating the AC cooling loop during cool-down (CD).

The RT factor for the ML-simulation is:

- $RT = 5.44 \times 10^{-6}$

Note that the ML-simulation does not attempt to simulate the cooling loop but does simulate different parts of the car cabin (driver and passenger's head, torso and foot).

Based on the above results, the speed-up for the ML-simulator compared with the 1D simulation (during WU) is 1400-fold.

### 5.3 Comparative performance in terms of capability

The two simulators have different sets of capabilities and this should be taken into account when considering other performance aspects.

The ML simulator has certain capabilities that are not available in the 1D simulator:

- It can provide properties needed to make use of the DOMUS Holistic Comfort Model (HCM) for both front bench occupants. Specifically, it estimates, for both occupants, temperature, mean radiant temperature, air velocity at head, torso, and foot.
- It can provide properties needed for estimating safety in terms of windshield fogging. Specifically, it estimates windshield glass temperature and relative humidity.

The 1D simulator, on the other hand, has capabilities not available in the ML simulator:

- It simulates the HVAC system more fully, including the AC loop, rather than requiring the air vent temperature as input. Note that the ML simulator does simulate the blower.
- It is a physics-based simulation and thus is likely to generalise more readily to circumstances not seen in the CWT trials.
- It supports additional DOMUS components, such as the radiant panels.

## 5.4 Summary

The 1D-simulator and ML simulator have similar accuracy, the ML-simulator is significantly faster to compute.

The capabilities of the two simulators are somewhat different and thus the selection of simulator needs to take this into account.

## 6 Conclusions (CRF / COV)

The ML simulator is sufficiently fast and accurate to suggest that this is a promising method. The 1D simulator, being physics-based, may still be preferred for some applications.

In order to make use of the ML simulator, additional work is needed, as follows:

1. A separate simulation of the HVAC system is needed to provide vent outlet temperatures. IDIADA have already done some investigation into producing such a simulation.
2. To properly simulate DOMUS components, such as the radiant panels, further simulation data are needed. This data might be produced based on the CFD simulation provided by IKA, for example.

In order to make use of the 1D simulator, some further work is also needed, as follows:

1. A way to provide fogging information will be required.
2. A way to estimate inputs to the Holistic Comfort Model is needed.

## 7 Recommendation

- The machine-learnt simulator is promising and should be adopted where possible. Specifically, it is computationally fast and the average accuracy is 1.8% (NRMSE).
- The 1D simulator provides a robust model with similar accuracy and, in particular, is able to deal with all the DOMUS features (such as, new HVAC, radiant panels, insulation) without any other calibration.
- Further improvement of the ML-simulator is possible by enlarging the available training dataset and including variation over DOMUS active and passive components. This is specifically needed to support WP2.3.
- For the ML simulator, a separate simulation of the HVAC system is needed to fully enable using it for optimisation within WP2 and WP5.
- If the 1D simulator is used instead, some solution will be needed to estimate fogging and comfort.

## 8 Risk register

Risk No.	What is the risk	Probability of risk occurrence <sup>2</sup>	Effect of risk <sup>3</sup>	Solutions to overcome the risk
<b>WP1.4.1</b>	Simulator does not perform sufficiently accurately under conditions other than those examined during CWT trials	Medium	High	Either revert to 1D simulator or consider adding further data to refine ML simulator
<b>WP1.4.2</b>	Missing simulation elements – HVAC must still be simulated to go from controls to vent temperatures	Low	High	IDIADA already have a simulator of this element but possibly an ML version could also be produced
<b>WP1.4.3</b>	Missing simulation of DOMUS components	Medium	High	IDIADA / ika are producing alternative CFD-based data-sets to learn a ML simulation from that will support these. Alternatively, work will need to proceed with a reduced set of components.

<sup>2</sup> Probability risk will occur: 1 = high, 2 = medium, 3 = Low

<sup>3</sup> Effect when risk occurs: 1 = high, 2 = medium, 3 = Low

## 9 References

Home - Keras Documentation. (n.d.). Retrieved April 27, 2020, from <https://keras.io/>

Kamar, H. M., Ahmad, R., Kamsah, N., Kamsah, N. B., Faiz, A., & Mustafa, M. (2012). Artificial neural networks for automotive air-conditioning systems performance prediction. *Elsevier*. <https://doi.org/10.1016/j.applthermaleng.2012.05.032>

Ng, B. C., Darus, I. Z. M., Jamaluddin, H., & Kamar, H. M. (2014). Dynamic modelling of an automotive variable speed air conditioning system using nonlinear autoregressive exogenous neural networks. *Applied Thermal Engineering*, 73(1), 1255–1269. <https://doi.org/10.1016/j.applthermaleng.2014.08.043>

Nowotny, T. (2014). Two Challenges of Correct Validation in Pattern Recognition. *Frontiers in Robotics and AI*, 1, 5. <https://doi.org/10.3389/frobt.2014.00005>

TensorFlow. (n.d.). Retrieved April 27, 2020, from <https://www.tensorflow.org/>

## 10 Acknowledgement

The author(s) would like to thank the partners in the project for their valuable comments on previous drafts and for performing the review.

### Project partners:

#	Partner	Partner Full Name
1	IDIADA	IDIADA AUTOMOTIVE TECHNOLOGY SA
2	CRF	CENTRO RICERCHE FIAT SCPA
3	TME	TOYOTA MOTOR EUROPE
4	Volvo Cars	VOLVO PERSONVAGNAR AB
5	AGC	AGC GLASS EUROPE SA
6	DNTS	DENSO Thermal Systems S.p.A.
7	Faurecia	Faurecia Sièges d'Automobile
8	HUTCH	HUTCHINSON SA
9	IEE	IEE International Electronics & Engineering S.A.
10	LIST	LUXEMBOURG INSTITUTE OF SCIENCE AND TECHNOLOGY
11	COV	COVENTRY UNIVERSITY
12	Fraunhofer	FRAUNHOFER GESELLSCHAFT ZUR FOERDERUNG DER ANGEWANDTEN FORSCHUNG E.V.
13	IKA	RHEINISCH-WESTFAELISCHE TECHNISCHE HOCHSCHULE AACHEN
14	TECNALIA	FUNDACION TECNALIA RESEARCH & INNOVATION
15	VIF	Kompetenzzentrum - Das Virtuelle Fahrzeug, Forschungsgesellschaft mbH
16	UNR	UNIRESEARCH BV



*This project has received funding from the European Union's Horizon 2020 research and innovation programme under Grant Agreement no. 769902*

## 11 Appendix A – Quality Assurance

The following questions should be answered by all reviewers (WP Leader, peer reviewer 1, peer reviewer 2 and the technical coordinator) as part of the Quality Assurance Procedure. Questions answered with NO should be motivated. The author will then make an updated version of the Deliverable. When all reviewers have answered all questions with YES, only then the Deliverable can be submitted to the EC.

NOTE: For public documents this Quality Assurance part will be removed before publication.

Question	WP Leader	Peer reviewer 1	Technical Coordinator
	J Brusey	S. Möller	IDIADA
<b>1. Do you accept this deliverable as it is?</b>	Yes	Yes	Yes
<b>2. Is the deliverable completely ready (or are any changes required)?</b>	Yes	Yes	Yes
<b>3. Does this deliverable correspond to the DoW?</b>	Yes	Yes	Yes
<b>4. Is the Deliverable in line with the DOMUS objectives?</b>	Yes	Yes	Yes
<b>a. WP Objectives?</b>	Yes	Yes	Yes
<b>b. Task Objectives?</b>	Yes	Yes	Yes
<b>5. Is the technical quality sufficient?</b>	Yes	Yes	Yes